

Fig. 5 BMP-2 enhances the canonical Wnt signal pathway. (A) Keratinocytes were seeded at 4.0×10^4 per well in 12-well collagen-coated dishes, and cultured in 1 mL of MCDB153 medium with BHE. After 48 h, the medium was replaced with 1 mL of fresh MCDB153 without BHE, and 0.5 µg of TOPFLASH and 10 ng of pRL-CMV were transfected. After a 10-h transfection of the reporter gene, the medium was replaced with 1 mL of fresh MCDB153 without BHE. Various concentrations of conditioned medium of L cells that expressed the Wnt-3a gene or neomycin (control vector) were added to the medium, and the cells were incubated for 72 h. Cells were harvested, and luciferase activity was measured. The luciferase activity of each sample was normalized against that of a non-stimulated sample. (B) Keratinocytes were cultured as described above, and transfected with 0.5 µg of TOPFLASH or FOPFLASH and 10 ng of pRL-CMV. After a 10-h transfection of the reporter gene, the medium was replaced with 1 mL of fresh MCDB153 without BHE. Various concentrations of BMP-2 were added to the medium and the cells were incubated for 72 h. The luciferase activity of each sample was normalized against that of a TOPFLASH-transfected, non-stimulated sample. (C) Keratinocytes were cultured as described above, and transfected with 0.5 µg of TOPFLASH and 10 ng of pRL-CMV. After a 10-h transfection of the reporter gene, the medium was replaced with 1 mL of fresh MCDB153 without BHE. BMP-2 (4 ng mL⁻¹) was added to the medium 24, 36, and 48 h before the cells were harvested, and luciferase activity was measured. The luciferase activity of each sample was normalized against that of a non-stimulated sample. (D) Keratinocytes were cultured as described above, and transfected with 0.5 µg of TOPFLASH and 10 ng of pRL-CMV. After a 10-h transfection of the reporter gene, the medium was replaced with 1 mL of fresh MCDB153 without BHE. BMP-2 (4 ng mL⁻¹) in combination with conditioned medium (5 ng mL⁻¹) of L cells that expressed the Wnt-3a gene or neomycin (control vector) were added to the medium, and the cells were incubated for 72 h. The luciferase activity of each sample was normalized against that of a non-stimulated sample. The bars and error bars represent the mean and S.D. of three independent experiments ($p < 0.05$ and $**p < 0.01$).

4. Discussion

By definition, both BMP-2 and Wnts are morphogens that specify different cell fates in concentration-dependent manners [18]. BMP-2 could induce epidermal fate of ectodermal cells during embryogenesis, and regulate hair follicle development [19–21]. Several reports revealed the roles of Wnts, Frizzleds, and β -catenin in regulating skin and hair development which suggested Wnt/ β -catenin pathway might be involved [22–24]. In our experiment, Wnt-2b/13, -4, -5a, -5b, -7a, -7b, and -10a mRNAs were detected in keratinocytes, and BMP-2 increased Wnt-2b/13, and

decreased Wnt-10a. Wnt-5b and -7a increased transiently soon after BMP-2 stimulation, and later decreased (Fig. 1). Interestingly, although BMP-2 did not decrease Wnt-4 expression in the confluent condition, BMP-2 suppressed cell density-dependent Wnt-4 induction (Figs. 1 and 3). In contrast, BMP-2 increased Wnt-2b/13 in both the confluent and subconfluent conditions (Figs. 1 and 3). These results suggest that BMP-2 modulates Wnt expression in keratinocytes, and cell confluence affects BMP-2-dependent Wnt induction. BMP-2 modulates the expression of Wnt-3a and -7a mRNA, and BMP-2 can upregulate the activity of *lef1* in the murine

multipotent mesenchymal cell line C3H10T1/2 [9,10]. In hair budding, however, BMP induces E-cadherin by suppressing Lef1 activation, and the balance between the BMP and Wnt signals regulates proper hair budding [25]. Therefore, cell types and cell conditions, such as proliferation, differentiation, and the cell environment, may influence the interaction between BMP-2 and Wnt.

In the frizzled family, BMP-2 increased frizzled-6 in a time-dependent manner, and transiently increased frizzled-8 and -10 (Fig. 2). These results suggest that BMP-2-treated keratinocytes are susceptible to Wnt stimulation. Interestingly, human keratinocytes express abundant SFRP-1/SARP-2 mRNA, and BMP-2 suppressed SFRP-1/SARP-2 expression (Fig. 2). SFRP/SARP mRNAs encode secreted proteins that possess a cysteine-rich domain homologous to those of frizzled proteins, but lack the transmembrane regions that are characteristic of frizzled-like proteins. It has been suggested that SFRP/SARPs bind to Wnt and interfere with the interaction between Wnt and frizzled, resulting in Wnt signal suppression, because SFRP-1/SARP-2 decreases the intracellular β -catenin concentration in cultured human breast adenocarcinoma MCF7 cells [26]. The increases in frizzled-6, -8, and -10, and the decrease in SFRP-1/SARP-2 by BMP-2 suggest that frizzled-6, -8, and -10, and SFRP-1/SARP-2 enhance the Wnt signaling pathway with BMP-2 stimulation in a coordinated manner.

TCF/LEF members, originally cloned as lymphoid transcription factors, are recognized as potent transactivators on interaction with β -catenin, the downstream target of Wnt signaling [27]. BMP-2 upregulated the transcriptional activity of TCF/LEF in human keratinocytes, and BMP-2 enhanced Wnt-3a-dependent TCF/LEF activation (Fig. 5). BMP-2 upregulated the expression of some members, such as Wnt-2b/13 and frizzled-6, which suggests that these Wnt and frizzled genes are involved in the subsequent activation of TCF/LEF in human keratinocytes. Other mechanisms may also be involved in BMP-2-dependent TCF/LEF activation. The BMP-2 signal is transduced by the smad family, and smad4 interacts with TCF/LEFs directly [28]. Thus, smad4, which is activated by BMP-2 signaling and translocated into the nucleus, may activate TCF/LEF directly, and support Wnt-3a-dependent TCF/LEF activation. At the least, BMP-2 enhanced the canonical Wnt pathway in normal human keratinocytes under certain conditions. However, 10 ng mL^{-1} of BMP-2 did not activate the canonical Wnt pathway (Fig. 5B). This may be the effect of keratinocyte differentiation because 10 ng mL^{-1} of BMP-2 induced morphological changes in some genes that are induced in differentiated keratinocytes

(unpublished data). Cell differentiation affects the expression of some Wnt, frizzled, and TCF/LEF genes [7,8,29]. Therefore, strong BMP-2 stimulation induces keratinocyte differentiation, and may not enhance TOPFLASH luciferase activity.

The particular stem cell lineage and stage of differentiation of the skin cell may influence the cell response to Wnt/ β -catenin signaling. Mutated β -catenin without transcriptional activity acts in epidermis to promote hair fate and in hair cells to promote epidermal fate [30]; skin stem cells fail to differentiate into follicular KC in the absence of β -catenin, but instead adopt an epidermal fate [22]. In cultured normal human keratinocytes, we showed BMP-2 modulates the expression of molecules related to Wnt signaling and activates the canonical Wnt pathway, and Wnt signaling may be affected by the fate of keratinocytes, such as their proliferation, migration and differentiation. However, the target genes of TCF/LEF activated by BMP-2 in normal human keratinocytes are not clear. It is our future concern to reveal the target genes and the downstream biological/cellular events which might be influenced by these target genes in normal human keratinocytes.

In conclusion, BMP-2 modulates the expression of molecules related to Wnt signaling and activates the canonical Wnt pathway in normal human keratinocytes. Moreover, Wnt signaling may be affected by the fate of keratinocytes, such as their proliferation, migration, and differentiation.

Acknowledgments

This work was partly supported by Health Sciences Research Grants for Research on Specific Diseases from the Ministry of Health, Labor, and Welfare of Japan and a Grant-in-Aid for Scientific Research from the Ministry of Education, Culture, Sports, Science, and Technology of Japan. We thank Teruko Tsuda and Eriko Tan for technical assistance.

References

- [1] Cadigan KM, Nusse R. Wnt signaling: a common theme in animal development. *Genes Dev* 1997;11:3286–305.
- [2] Miller JR. The Wnts. *Genome Biol* 2002;3 [REVIEWS3001, Epub 2001 December 28].
- [3] Huelsken J, Birchmeier W. New aspects of Wnt signaling pathways in higher vertebrates. *Curr Opin Genet Dev* 2001;11:547–53.
- [4] van Gijn ME, Snel F, Cleutjens JP, Smits JF, Blankesteyn WM. Overexpression of components of the Frizzled–Dishevelled cascade results in apoptotic cell death, mediated by β -catenin. *Exp Cell Res* 2001;265:46–53.

- [5] Behrens J. Control of beta-catenin signaling in tumor development. *Ann N Y Acad Sci* 2000;910:21–33.
- [6] Kishimoto J, Burgeson RE, Morgan BA. Wnt signaling maintains the hair-inducing activity of the dermal papilla. *Genes Dev* 2000;14:1181–5.
- [7] Saitoh A, Hansen LA, Vogel JC, Udey MC. Characterization of Wnt gene expression in murine skin: possible involvement of epidermis-derived Wnt-4 in cutaneous epithelial–mesenchymal interactions. *Exp Cell Res* 1998;243:150–60.
- [8] Hung BS, Wang XQ, Cam GR, Rothnagel JA. Characterization of mouse Frizzled-3 expression in hair follicle development and identification of the human homolog in keratinocytes. *J Invest Dermatol* 2001;116:940–6.
- [9] Dassule HR, McMahon AP. Analysis of epithelial–mesenchymal interactions in the initial morphogenesis of the mammalian tooth. *Dev Biol* 1998;202:215–27.
- [10] Fischer L, Boland G, Tuan RS. Wnt signaling during BMP-2 stimulation of mesenchymal chondrogenesis. *J Cell Biochem* 2002;84:816–31.
- [11] Suzuki A, Kaneko E, Ueno N, Hemmati-Brivanlou A. Regulation of epidermal induction by BMP2 and BMP7 signaling. *Dev Biol* 1997;189:112–22.
- [12] Shirakata Y, Tokumaru S, Yamasaki K, Sayama K, Hashimoto K. So-called biological dressing effects of cultured epidermal sheets are mediated by the production of EGF family, TGF-beta and VEGF. *J Dermatol Sci* 2003;32:209–15.
- [13] Shirakata Y, Ueno H, Hanakawa Y, Kameda K, Yamasaki K, Tokumaru S, et al. TGF-beta is not involved in early phase growth inhibition of keratinocytes by 1alpha,25(OH)2Vitamin D3. *J Dermatol Sci* 2004;36:41–50.
- [14] Shibamoto S, Higano K, Takada R, Ito F, Takeichi M, Takada S. Cytoskeletal reorganization by soluble Wnt-3a protein signalling. *Genes Cells* 1998;3:659–70.
- [15] Yamasaki K, Hanakawa Y, Tokumaru S, Shirakata Y, Sayama K, Hanada T, et al. Suppressor of cytokine signaling 1/JAB and suppressor of cytokine signaling 3/cytokine-inducible SH2 containing protein 3 negatively regulate the signal transducers and activators of transcription signaling pathway in normal human epidermal keratinocytes. *J Invest Dermatol* 2003;120:571–80.
- [16] Huguet EL, Smith K, Bicknell R, Harris AL. Regulation of Wnt5a mRNA expression in human mammary epithelial cells by cell shape, confluence, and hepatocyte growth factor. *J Biol Chem* 1995;270:12851–6.
- [17] Zhu AJ, Watt FM. Beta-catenin signalling modulates proliferative potential of human epidermal keratinocytes independently of intercellular adhesion. *Development* 1999;126:2285–98.
- [18] Christian JL. BMP, Wnt and Hedgehog signals: how far can they go? *Curr Opin Cell Biol* 2000;12:244–9.
- [19] Botchkarev VA, Botchkareva NV, Sharov AA, Funa K, Huber O, Gilchrist BA. Modulation of BMP signaling by noggin is required for induction of the secondary (nonyltoch) hair follicles. *J Invest Dermatol* 2002;118:3–10.
- [20] Qiao W, Li AG, Owens P, Xu X, Wang XJ, Deng CX. Hair follicle defects and squamous cell carcinoma formation in Smad4 conditional knockout mouse skin. *Oncogene* 2005.
- [21] Suzuki A, Kaneko E, Ueno N, Hemmati-Brivanlou A. Regulation of epidermal induction by BMP2 and BMP7 signaling. *Dev Biol* 1997;189:112–22.
- [22] Huelsenken J, Vogel R, Erdmann B, Cotsarelis G, Birchmeier W. Beta-catenin controls hair follicle morphogenesis and stem cell differentiation in the skin. *Cell* 2001;105:533–45.
- [23] Reddy S, Andl T, Bagasra A, Lu MM, Epstein DJ, Morrisey EE, et al. Characterization of Wnt gene expression in developing and postnatal hair follicles and identification of Wnt5a as a target of Sonic hedgehog in hair follicle morphogenesis. *Mech Dev* 2001;107:69–82.
- [24] Reddy ST, Andl T, Lu MM, Morrisey EE, Millar SE. Expression of Frizzled genes in developing and postnatal hair follicles. *J Invest Dermatol* 2004;123:275–82.
- [25] Jamora C, DasGupta R, Kocieniewski P, Fuchs E. Links between signal transduction, transcription and adhesion in epithelial bud development. *Nature* 2003;422:317–22.
- [26] Melkonyan HS, Chang WC, Shapiro JP, Mahadevappa M, Fitzpatrick PA, Kiefer MC, et al. SARPs: a family of secreted apoptosis-related proteins. *Proc Natl Acad Sci USA* 1997;94:13636–41.
- [27] Roose J, Clevers H. TCF transcription factors: molecular switches in carcinogenesis. *Biochim Biophys Acta* 1999;1424:M23–37.
- [28] Pukrop T, Gradl D, Henningfeld KA, Knochel W, Wedlich D, Kuhl M. Identification of two regulatory elements within the high mobility group box transcription factor XTcf-4. *J Biol Chem* 2001;276:8968–78.
- [29] Zhou P, Byrne C, Jacobs J, Fuchs E. Lymphoid enhancer factor 1 directs hair follicle patterning and epithelial cell fate. *Genes Dev* 1995;9:700–13.
- [30] DasGupta R, Rhee H, Fuchs E. A developmental conundrum: a stabilized form of beta-catenin lacking the transcriptional activation domain triggers features of hair cell fate in epidermal cells and epidermal cell fate in hair follicle cells. *J Cell Biol* 2002;158:331–44.

Available online at www.sciencedirect.com

SCIENCE @ DIRECT®

Identification of Human Oral Keratinocyte Stem/Progenitor Cells by Neurotrophin Receptor p75 and the Role of Neurotrophin/p75 Signaling

TAKAHIRO NAKAMURA,^{a,b} KEN-ICHI ENDO,^a SHIGERU KINOSHITA^a

^aDepartment of Ophthalmology, Kyoto Prefectural University of Medicine, Graduate School of Medicine, Kyoto, Japan; ^bResearch Center for Regenerative Medicine, Doshisha University, Kyoto, Japan

Key Words. p75 • Oral mucosa • Keratinocyte • Stem cell • Clonal analysis • Neurotrophin

ABSTRACT

This study was undertaken to determine whether human oral keratinocyte stem cells characteristically express higher levels of the low-affinity neurotrophin receptor p75 and to elucidate the function of p75 in oral keratinocytes. Examination of their expression patterns and cell-cycling status in vivo showed that p75 was exclusively expressed in the basal cell layer of both the tips of the papillae and the deep rete ridges. These immunostaining patterns suggest a cluster organization; most p75(+) cells did not actively cycle in vivo. Cell sorting showed that cells in the p75(+) subset were smaller and possessed higher in vitro proliferative capacity and clonal growth potential than the p75(-) subset. Clonal analysis revealed that holoclone-type (stem cell compart-

ment), meroclone-type (intermediate compartment), and paraclone-type (transient amplifying cell compartment) cells, previously identified in skin and the ocular surface, were present in human oral mucosal epithelium. Holoclone-type cells showed stronger p75 expression at both the mRNA and protein level than did meroclone- and paraclone-type cells. Among the several neurotrophins, nerve growth factor (NGF) and neurotrophin-3 stimulated p75(+) oral keratinocyte cell proliferation, and only NGF protected them from apoptosis. Our in vivo and in vitro findings indicate that p75 is a potential marker of oral keratinocyte stem/progenitor cells and that some neurotrophin/p75 signaling affects cell growth and survival. *STEM CELLS* 2007;25:628–638

INTRODUCTION

Epithelial cells, such as epidermal, esophageal, corneal, and oral keratinocytes, are organized into multiple layers. Like other rapidly renewing tissues, such as the hemopoietic system, the human epithelium is constantly regenerating. In general, proliferation occurs in the basal layer of keratinocytes attached to the underlying basement membrane; cells that undergo terminal differentiation as they migrate through the suprabasal layers are shed from the tissue surface [1]. Stem cells (SCs) facilitate the maintenance of self-renewing tissues; they are critical for replenishing and maintaining the cell balance (homeostasis) within tissues and for regenerating damaged tissue. Based on previous studies of several tissue types, criteria for keratinocyte SCs prescribe that they are relatively undifferentiated both ultrastructurally and biochemically; retain a high capacity for long-term, error-free self-renewal; have high proliferative potential; cycle slowly or rarely in vivo; are stimulated to proliferate in response to injury and certain growth stimuli; and are usually found in well-protected, highly vascularized and innervated areas [2–6]. It is generally known that SCs infrequently divide, yet they can proliferate soon in response to injury and certain growth stimuli, resulting in one SC and one transient amplifying cell (TAC) with limited proliferative potential. TACs are responsible for most routine proliferative activities; they are capable of extensive expansion of the cell population [7,

8]. Upon exhaustion of their proliferative potential, the rapidly proliferating TACs undergo terminal differentiation.

In this study, we used clonal analysis and cell sorting techniques for the purpose of characterizing the tissue SC and TAC populations. Clonal analysis identified three types of keratinocytes with different capacities for multiplication in human epidermis, hair follicles, and ocular surface epithelium [9–11]. Holoclones have the highest reproductive capacity, in paraclones, all cells undergo terminal differentiation within a few generations, and the behavior of meroclones is intermediate between holoclones and paraclones. Holoclones, meroclones, and paraclones are considered to be SCs, young TACs, and TACs, respectively. The holoclone-meroclone-paraclone transition is a unidirectional process that occurs during natural cell aging and during repeated subcultivation.

The cell-sorting technique uses phenotypic cell surface markers that distinguish differentiated cells from progenitor cells. Interesting results have been obtained in several tissue types. In human epidermis, SCs could be distinguished from differentiated keratinocytes by their higher expression of $\beta 1$ integrins [12, 13] and the combination of high levels of $\alpha 6$ integrin and low-to-undetectable levels of the transferring receptor (CD71) [14, 15]. For the further molecular characterization of various keratinocyte SCs, additional cell surface markers are needed.

The human oral cavity contains masticatory mucosa, such as gingiva, and lining mucosa, such as buccal mucosa. Oral mucosal epithelium has drawn attention as a cell source for a

Correspondence: Takahiro Nakamura, M.D., Ph.D., Department of Ophthalmology, Kyoto Prefectural University of Medicine, Kawaramachi Hirokoji, Kamigyo-ku, Kyoto 602-0841, Japan. Telephone: 81-75-251-5578; Fax: 81-75-251-5663; e-mail: tnakamur@ophth.kpu-m.ac.jp
Received August 7, 2006; accepted for publication November 9, 2006; first published online in *STEM CELLS EXPRESS* November 16, 2006.
©AlphaMed Press 1066-5099/2007/\$30.00/0 doi: 10.1634/stemcells.2006-0494

STEM CELLS 2007;25:628–638 www.StemCells.com

variety of tissue-engineered reconstructions, such as oral cavity [16], epidermis [17], and especially ocular surface reconstruction [18–23], and the transplantation of human oral epithelial sheets grown on various substrates can be useful for tissue reconstruction. In the clinical setting, the quality of the cultivated graft is the key to success, and the selection of a large number of highly proliferating oral epithelial cells, such as SCs and TACs, enhances the reproducibility, quality, and longevity of these grafts. However, little is known about oral keratinocyte SCs and TACs.

The p75 molecule, a low-affinity neurotrophin receptor, is a member of the tumor necrosis factor receptor superfamily [24]; its function is to mediate cell survival, apoptosis, and intercellular signaling in neuronal tissues [25, 26]. There is experimental evidence that p75 is also involved in controlling the fate of murine keratinocyte SCs through cell-cell interactions [27] and that it characterizes esophageal keratinocyte SCs in vitro [28]. However, its function in various human keratinocyte SCs remains to be fully elucidated.

We investigated the fate of p75(+) cells to determine whether this subset is critical for stem- or progenitor-cell lineages in human oral keratinocytes. Using clonal analysis and cell sorting, we evaluated the p75 expression patterns of human oral mucosal tissue and attempted to identify and isolate human oral keratinocyte stem/progenitor cells. We then investigated the effect of neurotrophin/p75 signaling in isolated oral keratinocytes. We found that human oral keratinocyte stem/progenitor cell phenotypes are characterized by their expression of p75 and that some neurotrophin/p75 signaling affected cell proliferation and survival.

MATERIALS AND METHODS

Tissues

Oral tissues were obtained from healthy volunteers and as superfluous tissue from patients undergoing oral surgery. We followed the tenets of the Declaration of Helsinki; all donors provided proper informed consent for biopsy. All samples were processed within 1–2 hours of harvest.

Cell Culture

For culture of the human oral epithelial cells, we used our previously reported system [18–20]. Briefly stated, submucosal connective tissues were removed with scissors to the extent possible; the resulting samples were cut into small explants. These were incubated (37°C, 1 hour) with 1.2 IU of Dispase (Roche, Indianapolis, <http://www.roche.com>) and treated with 0.05% trypsin-EDTA solution (10 minutes, room temperature) to separate the cells. The cell suspension was filtered through a cell dissociation sieve (Sigma-Aldrich, St. Louis, <http://www.sigmaaldrich.com>) to remove unsatisfactory segments; this yielded a suspension of purified oral epithelial cells. Isolated cell suspensions were then subjected to cell-sorting assay and clonal analysis.

Clonal Analysis

For clonal analysis, we applied the method of Barrandon and Green [9]. Secondary cultures of oral epithelial cells were used. Briefly stated, single cells, isolated under an inverted microscope, were inoculated into 12-well plates that contained a feeder layer of mitomycin C (MMC)-inactivated NIH-3T3 fibroblasts. After 7 days, a single clone was identified under an inverted microscope and photographed. Each clone was then divided into three parts; 5/8 of the clone was used for real-time polymerase chain reaction (PCR) assay, and 1/8 was subjected to immunocytochemical analysis to evaluate the cell characteristics. The other 1/4 of the clone was transferred to an indicator dish, fixed 10–12 days later, and stained with 0.1% toluidine blue for classification of the clonal type, which

was determined by the percentage of aborted colonies [9]. When 0%–5% of the colonies were terminal, the clone was classified as a holoclone. When all colonies were terminal or when no colonies formed, the clone was classified as a paraclone, and when >5% but <100% of the colonies were terminal, the clone was classified as a meroclone.

Antibodies and Reagents

The following mouse monoclonal antibodies (mAbs) were used: anti-p75 (dilution, ×200) (Chemicon, Temecula, CA, <http://www.chemicon.com>; Abcam, Cambridge, U.K., <http://www.abcam.com>; and Upstate Biotech, Lake Placid, NY, <http://www.upstate.com>), anti-desmoplakin (×1) (Progen, Heidelberg, Germany, <http://www.progen.de>), anti-keratin 4 (×200)/10 (×50)/13 (×200) (Novocastra Ltd., Newcastle upon Tyne, U.K., <http://www.novocastra.co.uk>), anti-integrin $\alpha 6$ (×200)/ $\beta 4$ (×500)/ $\alpha 3$ (×50)/ $\beta 1$ (×500) (Chemicon), CD34 (×50) (BD Biosciences, San Diego, <http://www.bdbiosciences.com>), CD71 (×50) (YLEM, Roma, Italy, <http://www.ylem.it>), BCRP (×10) (Kamiya Biomedical, Seattle, <http://kamiyabiomedical.com/>), and anti-Ki67 (×100) (Dako, Kyoto, Japan, <http://www.dako.com>). Rabbit polyclonal antibodies were also used: anti-ZO1 (×25) (Zymed, South San Francisco, CA, <http://www.invitrogen.com>) and anti-Ki67 (×50) (Abcam). Secondary antibodies were Alexa Fluor-488 goat anti-mouse or rabbit IgG (×1,500) and Alexa Fluor-594 goat anti-mouse or rabbit IgG (×1,500) (Molecular Probes Inc., Eugene, OR, <http://probes.invitrogen.com>). The following neurotrophins were used: nerve growth factor (NGF), brain-derived neurotrophic factor (BDNF), neurotrophin-3 (NT-3), and neurotrophin-4 (NT-4) (Sigma-Aldrich).

Cell Fractionation

The p75(+) and p75(–) cells were separated using magnetic cell sorting with the indirect microbead system (MACS; Miltenyi Biotec, Bergisch Gladbach, Germany, <http://www.miltenyibiotec.com>). The oral epithelial cell suspensions were labeled with anti-p75 mAb (×400) at 0°C for 15 minutes. The cells were then carefully washed with MACS buffer (phosphate-buffered saline [PBS] supplemented with 2 mM EDTA and 0.5% bovine serum albumin), incubated with rat anti-mouse IgG₁ microbeads (×5) at 4°C for 15 minutes, and exposed to the magnetic field of a permanent magnet on columns containing a ferromagnetic matrix. To increase the purity of the positive fraction, our protocol combined depletion columns and positive selection columns.

Validation of the Cell-Sorting Procedure

Flow Cytometry and Immunofluorescence. After the MACS procedure, each p75(+) and p75(–) cell fraction was again washed with MACS buffer and stained with Alexa Fluor-488 goat anti-mouse IgG (×1,500) at 4°C for 20 minutes for subsequent flow cytometric analysis (FACSCalibur; BD Biosciences) and immunofluorescence study. The cells were coverslipped using antifading mounting medium and examined under an immunofluorescence microscope (Olympus, Tokyo, <http://www.olympus-global.com>).

Reverse Transcription PCR. Total RNA was isolated from each isolated cell fraction using TRIzol reagent in accordance with the manufacturer's protocol. Complementary DNA was generated by mixing the extracted RNA (1 $\mu\text{g}/\mu\text{l}$ per sample) with a random hexamer primer and AMV Reverse Transcriptase XL (Takara, Tokyo, <http://www.takara.co.jp>). The primers and PCR conditions were followed the previously reported method [28]. The expected product sizes were 230 base pairs (bp) for p75 and 541 bp for β -actin.

Measurement of Cell Area

Each isolated cell fraction was centrifuged and resuspended in culture medium. Cells (approximately 10^3 cells) in 10 ml of medium were placed in 100-mm culture dishes and photographed under an inverted microscope using a ×10 phase objective [29]. Cell areas were measured randomly (200 cells per fraction) using Scion Image

software (Scion Corp., Frederick, MD, <http://www.scioncorp.com/>) and statistically analyzed.

5-Bromo-2'-deoxyuridine Cell Proliferation Assay

The proliferative capacity of each isolated cell fraction was determined by 5-bromo-2'-deoxyuridine (BrdU) enzyme-linked immunosorbent assay (ELISA) cell proliferation assay (Amersham Biosciences, Freiburg, Germany, <http://www.amersham.com>) using a previously reported protocol [20, 30]. Analysis was on the 6th day of passage ($n = 3$). Cultured cells were incubated with 10 μ M BrdU-labeling solution (20 hours, 37°C), washed with 250 μ l of PBS containing 10% serum per well, fixed with 70% ethanol in hydrochloric acid (30 minutes, -20°C), and incubated with 100 μ l of monoclonal antibody against BrdU (90 minutes), and then 100 μ l of peroxidase substrate was added to each well. BrdU absorbance in each well was measured directly with a spectrophotometric microplate reader at a test wavelength of 450 nm and a reference wavelength of 490 nm. This measure of the degree of cell proliferation we termed the proliferation index. Each sample was cultured in triplicate.

The proliferative capacity of isolated p75(+) cells incubated with several neurotrophins (NGF, NT-3, NT-4, and BDNF) was also analyzed using the same procedure. The p75(+) cells were seeded at a density of 2×10^5 cells per cm^2 for 48 hours. Next, the cells were preincubated with the aforementioned neurotrophins (1, 10, and 100 ng/ml, respectively) for an additional 48 hours and then analyzed.

Colony-Forming Efficiency

The clonal growth ability of each isolated cell fraction was determined by colony-forming efficiency (CFE) assay. Cells (2×10^5) were plated on six-well culture dishes that contained a feeder layer of MMC-inactivated NIH-3T3 fibroblasts ($n = 3$). The colonies were fixed on day 7, stained with 0.1% trydine blue, and counted independently by three investigators; the data were then averaged. Each sample was cultured in triplicate. CFE was defined as the ratio of the number of colonies to the number of viable cells seeded.

Ex Vivo Expansion of Isolated Cells

To culture isolated cell fractions we used our previously reported system [18–20]. Isolated cells (1×10^5 cells per well) were then seeded onto denuded amniotic membrane (AM) spread on the bottom of culture inserts, and cocultured for 10 days with mitomycin C-inactivated 3T3 fibroblasts (2×10^4 cells per cm^2). The culture medium consisted of a defined keratinocyte growth medium (ArBlast, Kobe, Japan, <http://www.arblast.jp>) supplemented with 5% fetal bovine serum. The percentage of Ki67(+) cells in the basal layer of cultivated epithelium was determined on tissue sections. We analyzed five different fields from samples obtained from three different donors (15 areas per donor).

Immunohistochemistry

Immunohistochemical studies followed our previously described method [18, 20]. Briefly stated, 3- μ m-thick cryostat sections were placed on gelatin-coated slides, air-dried, and rehydrated in PBS at room temperature for 15 minutes. To block nonspecific binding, the tissues were incubated with 2% bovine serum albumin (room temperature, 30 minutes). The sections were then incubated (room temperature, 1 hour) with the appropriate primary antibody (simple antibody or a mixture of antibodies for double staining) and washed (three times) in PBS containing 0.15% Triton X-100 for 15 minutes. Control incubations were with the appropriate normal mouse and rabbit IgG (Dako) at the same concentration as the primary antibody; the primary antibody for the respective specimen was omitted. After staining with the primary antibody, the sections were incubated with the appropriate secondary antibodies (room temperature, 1 hour), washed several times with PBS, coverslipped using antifading mounting medium containing propidium iodide or 4,6-diamidino-2-phenylindole (Vectashield; Vector Laboratories, Burlingame, CA, <http://www.vectorlabs.com>), and examined under a confocal microscope (Olympus Fluoview).

Real-Time PCR

Quantitative real-time PCR for p75, integrin β 1, integrin α 6, CD71, and ABCG2 was performed using an ABI Prism 7000 instrument (Applied Biosystems, Foster City, CA, <http://www.appliedbiosystems.com>). Total RNA was isolated with the RNeasy Micro Kit (Qiagen, Tokyo, <http://www1.qiagen.com>) ($n = 5$). We then performed quantitative real-time reverse transcription (RT)-PCR using QuantiTect Probe RT-PCR kits (Qiagen). Primers and probes for p75, integrin β 1, integrin α 6, CD71, ABCG2, and β -actin were from Applied Biosystems. For relative quantification, we used the ΔC_T method (Applied Biosystems). Analyses were performed in a sequence detector (ABI Prism 7000) using the accompanying data analysis software.

Apoptosis Assay

The p75(+) cells were seeded at a density of 2×10^5 cells per cm^2 on a chamber slide for 48 hours. Next, the cells were preincubated with several neurotrophins (100 ng/ml) for 48 hours, with or without UV irradiation (25 mJ per cm^2) [31]. The cells were directly stained by the In Situ Apoptosis Detection Kit (terminal deoxynucleotidyl transferase dUTP nick-end labeling [TUNEL] assay; Takara).

RESULTS

In Vivo Expression Patterns and Cell-Cycling Status of p75(+) Human Oral Keratinocytes

The in vivo expression patterns of p75 in human oral mucosal epithelium were investigated by indirect immunofluorescence. We used p75 antibodies from three companies (Chemicon, Abcam, and Upstate Biotech) and found no differences in the immunohistochemical results. We obtained tissues from the buccal mucosa (representing lining mucosa), where rete ridges are comparatively shallow and gentle, and gingiva (representing masticatory mucosa), where they are steep and deep. In the buccal mucosa, we noted intensive p75 expression primarily in the basal cell layer of the tips of the papillae (Fig. 1A); in some parts, p75 was expressed in deep rete ridges (Fig. 1B). In the gingiva, it was exclusively expressed in the basal cell layer of both the tips of the papillae and the deep rete ridges (Fig. 1C). In both tissues, p75 was expressed in the cell membrane. The immunostaining patterns suggest cluster (patch) organization, and clusters of brightly fluorescent basal cells were interspersed with stretches of basal cells with little or no fluorescence. The percentage of p75(+) cells per total oral keratinocytes was 7.35 ± 3.41 (five different fields from six different donors [total, 30 sections] were analyzed).

Slow or infrequent cycling is one of the unique features of adult SCs [32–37]. To investigate the in vivo cell cycle status in human oral mucosal epithelium, we used double immunostaining with p75 and Ki67, a marker for actively cycling cells. Ki67 was primarily expressed in the suprabasal and occasionally in the basal cell layer of oral epithelium (Fig. 1D, 1E). Statistical analysis of our double-staining results on 32 sections (5–10 sections each from four different donors) showed that among the p75(+) cells, the proportion of Ki67(–) cells was significantly higher ($96.63\% \pm 2.69\%$) than that of Ki67(+) cells ($3.37\% \pm 2.68\%$) (*, $p < .001$, t test), indicating that in vivo, most p75(+) cells were not actively cycling cells (Fig. 1F).

Characteristics of p75(+) and p75(–) Cell Fractions

To examine the characteristics of the p75(+) and p75(–) cell fractions, we isolated the subsets by magnetic cell sorting and validated our results by flow cytometry, RT-PCR, and immunofluorescence (supplemental online Fig. 1). Flow cytometric analysis showed that our use of a combination of depletion and positive selection columns yielded a purity in excess of 92% for

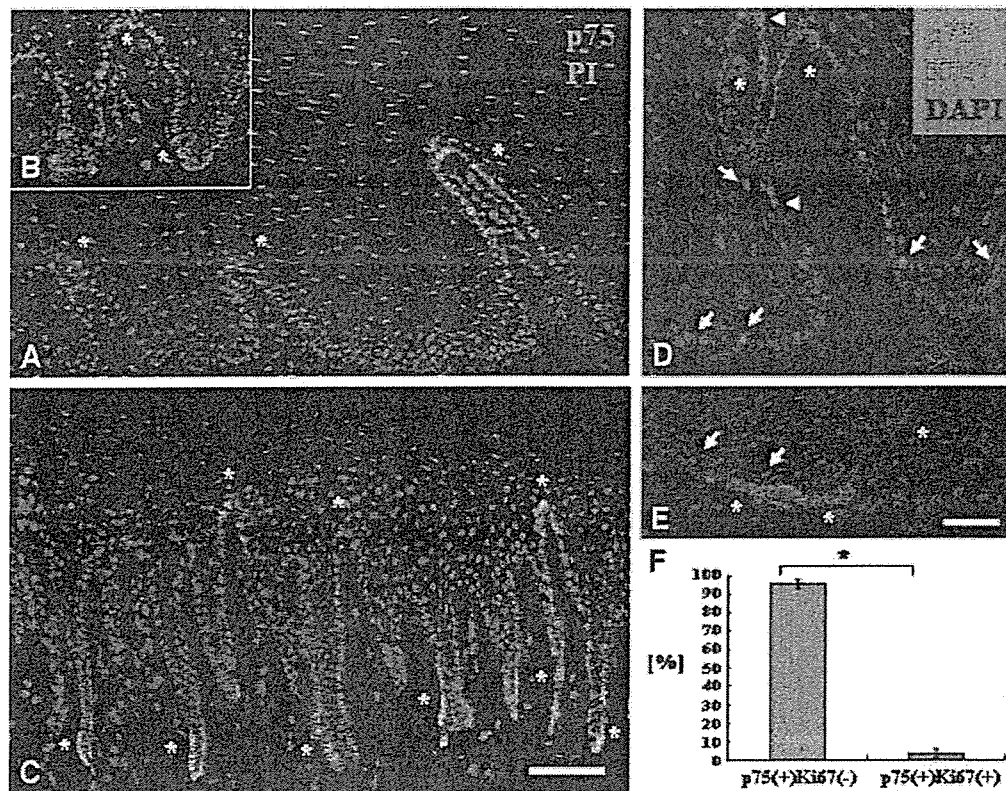


Figure 1. Immunolocalization of p75 and p75-Ki67 in human oral mucosal tissues. (A–C): In buccal mucosa, rete ridges are relatively shallow and gentle: p75 expression was intense primarily in the basal cell membrane of the tips of the papillae (A) (*). There was p75 expression in some deep rete ridges (B) (*). In the gingiva, rete ridges are deep and steep: p75 was expressed exclusively in the basal cell layer of the tips of the papillae and the deep rete ridges (C) (*). Patches of brightly fluorescent basal cells were interspersed with stretches of basal cells showing no or little fluorescence. (D–F): Ki67 expression was mainly observed in the suprabasal cell layer and occasionally in the basal cell layer of oral epithelium (D, E). The percentages of Ki67(–) and Ki67(+) cells among all p75(+) cells were $96.63\% \pm 2.69\%$ and $3.37\% \pm 2.68\%$, respectively (F). The difference was statistically significant (*, $p < .001$, *t* test). Asterisks and arrows indicate clusters of p75(+) and Ki67(+) cells, respectively. Arrowheads indicate p75(+) Ki67(+) cells. Scale bars = 100 μm . Abbreviations: DAPI, 4,6-diamidino-2-phenylindole; PI, propidium iodide.

p75(+) cells in all experiments (supplemental online Fig. 1A). RT-PCR and immunofluorescence for p75 confirmed its expression at both the mRNA and protein level in the purified fraction (supplemental online Fig. 1B, 1C).

As the highest clonogenicity, a feature of SCs, is reportedly found in the smallest keratinocytes [29], we measured the cell size in each isolated fraction using Scion Image software. Under an inverted microscope, p75(+) cells were clearly smaller than p75(–) cells (Fig. 2A). The average size of p75(+) cells was significantly smaller than that of p75(–) cells (102.52 ± 46.85 vs. $346.84 \pm 134.67 \mu\text{m}^2$; *, $p < .001$, *t* test) (Fig. 2A).

The proliferative capacity and clonal growth ability of each isolated cell fraction was determined by BrdU ELISA cell proliferation assay and CFE. Phase-contrast inspection of the isolated cells on the 6th day of passage showed that p75(+) cells formed colonies consisting of ovoid and round cells (Fig. 2B); p75(–) cells, which did not form colonies, were large and elongated (Fig. 2B). The proliferation indexes of p75(+) and p75(–) cell fractions were significantly different (9.64 ± 0.1 vs. 1.16 ± 0.09 ; *, $p < .001$, *t* test) (Fig. 2B), as was the CFE ($10.1\% \pm 1.2\%$ vs. $0.19\% \pm 0.07\%$; *, $p < .001$, *t* test) (Fig. 2C), indicating that the p75(+) fraction manifested greater in vitro proliferative capacity than the p75(–) fraction.

To evaluate their in vitro tissue-forming ability, we cultivated isolated cell fractions on an AM substrate. After 10 days of cultivation, p75(+) oral epithelial cells formed 4–5 layers exhibiting well-conserved columnar basal cells and

progressive flattening toward the surface (p75(+) sheet). On the other hand, p75(–) cells grew in monolayers composed of elongated, differentiated cells (Fig. 2D). To assess the cell-cycling status of these cultivated oral epithelial cells we examined their expression of Ki67. In p75(+) and p75(–) sheets, Ki67-labeled cells constituted $81.3\% \pm 10.6\%$ and $25.4\% \pm 9.9\%$, respectively (Fig. 2D), rendering the difference in the Ki67-labeling index statistically significant (*, $p < .001$, *t* test).

Using immunofluorescence and specific markers, we studied the morphological and biological characteristics of the p75(+) and p75(–) sheets. ZO-1, a tight junction-related component, was expressed in the apical surface on p75(+) but not p75(–) sheets (Fig. 3A, 3B). Desmoplakin, a cell-cell junction component, was clearly expressed in the cell membrane on p75(+) sheets; there was moderate desmoplakin expression on p75(–) sheets (Fig. 3C, 3D). On p75(+) sheets, nonkeratinized, mucosa-specific keratin 4 was expressed in the superficial layer and the upper half of the intermediate layer; keratin 13 was expressed in all but the basal cell layers (Fig. 3E, 3G). On p75(–) sheets, on the other hand, there was no or faint superficial staining (Fig. 3F, 3H). The basement membrane assembly proteins integrin $\alpha 6/\beta 4$ showed linear positive staining on the basement membrane side on both p75(+) and p75(–) sheets (Fig. 3I–3L). Integrin $\alpha 3$ was mainly expressed in the basal cell membrane on both p75(+) and p75(–) sheets (Fig. 3M, 3N), and

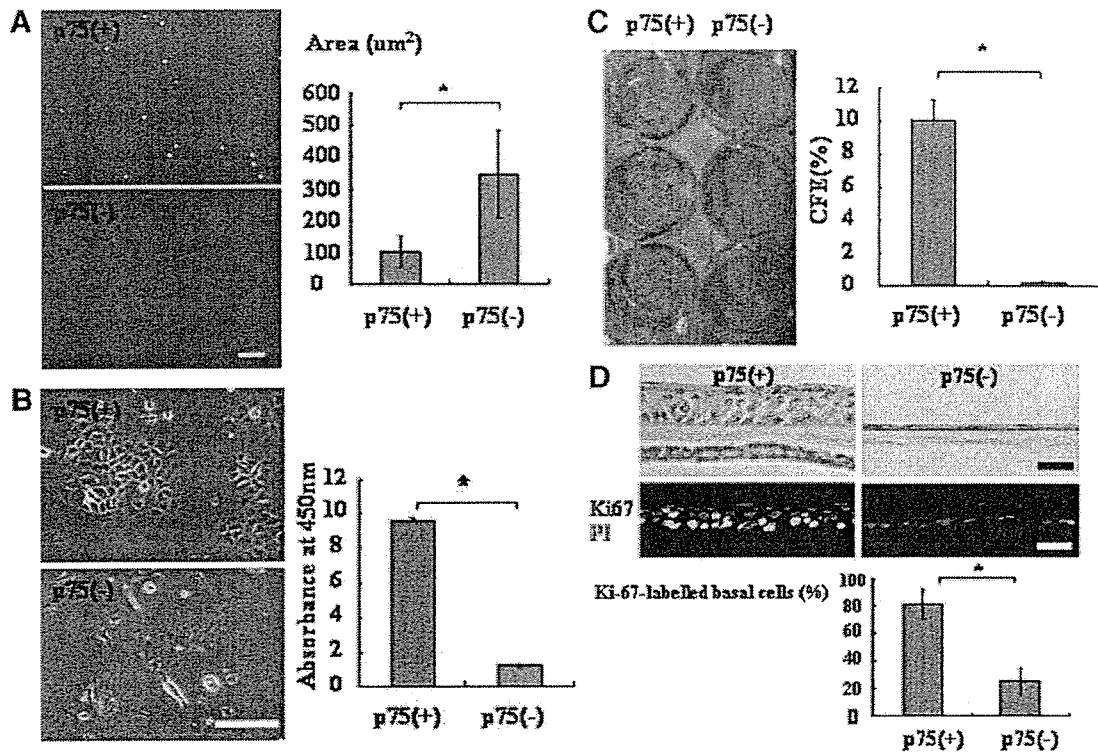


Figure 2. Characteristics of p75(+) and p75(-) cell fractions. (A): Under an inverted microscope, p75(+) cells are clearly smaller than p75(-) cells. The average cell size of the p75(+) cell fraction was $102.52 \pm 46.85 \mu\text{m}^2$, significantly smaller than the $346.84 \pm 134.67 \mu\text{m}^2$ of the p75(-) cell fraction (*, $p < .001$, *t* test). Scale bars = 100 μm . (B): Phase-contrast of isolated cells on the 6th day of passage. p75(+) cells formed colonies with ovoid and round cells; p75(-) cells did not form colonies and presented as large elongated cells. 5-Bromo-2'-deoxyuridine enzyme-linked immunosorbent assay showed that the proliferation indexes of p75(+) and p75(-) cell fractions was 9.64 ± 0.1 and 1.16 ± 0.09 , respectively. The difference was statistically significant (*, $p < .001$, *t* test). (C): The clonal growth ability of isolated cell fractions was determined by CFE assay. Cells (2×10^3) were plated on six-well culture dishes containing a feeder layer of mitomycin C-inactivated NIH-3T3 fibroblasts. Colonies were fixed on day 7 and stained with 0.1% trydine blue. The CFEs of p75(+) and p75(-) cells were $10.1\% \pm 1.2\%$ and $0.19\% \pm 0.07\%$, respectively, and the difference was statistically significant (*, $p < .001$, *t* test). (D): On the amniotic membrane (AM) substrate, p75(+) oral epithelial cells formed four to five layers. Note the well-conserved columnar basal cells and the progressive flattening toward the surface. Cultivated p75(-) cells grew in monolayers and consisted of elongated differentiated cells. Of the total basal cells in p75(+) and p75(-) sheets, $81.3\% \pm 10.6\%$ and $25.4\% \pm 9.9\%$, respectively, were Ki67-labeled. The difference in the Ki67-labeling index in the isolated cell fractions was statistically significant (*, $p < .001$, *t* test). Scale bars = 100 μm . Abbreviations: CFE, colony-forming efficiency; PI, propidium iodide.

integrin $\beta 1$ was expressed in the cell membrane of nearly all epithelial cells on p75(+) sheets; moderate or faint integrin $\beta 1$ staining was observed on p75(-) sheets (Fig. 3O, 3P). Thus, only the p75(+) sheets manifested normal cell differentiation and normal junctional specialization, suggesting that only the p75(+) cells possessed high in vitro proliferative capacities and normal three-dimensional (3D) tissue formation potential.

Isolation and Clonal Analysis of Oral Keratinocyte SCs

To determine whether holoclones, meroclones, and paraclones, previously identified in human epithelium [9–11, 38], are also present in human oral mucosal epithelium, we isolated single cells from eight different primary cultures obtained from eight different donors (four buccal mucosa, four gingiva). We analyzed 396 clones; of these, $56.9\% \pm 22.8\%$ formed original clones (Table 1). Photographs of representative holoclones, meroclones, and paraclones are shown in Figure 4. According to Barrandon and Green [9] and Pellegrini et al. [11], the representative original clone of the holoclone is large, has a smooth perimeter, and contains mainly small cells (Fig. 4A); most original clones of the paraclone are small and contain large differentiated squamous cells (Fig. 4C), and the meroclone is

intermediate between the holoclone and the paraclone (Fig. 4B). On indicator dishes, holoclones formed large, rapidly growing colonies, fewer than 5% of which aborted or terminally differentiated (Fig. 4D). The paraclone grew no colonies or only uniformly small, terminal colonies (Fig. 4F), and the meroclone formed growing and aborted colonies (Fig. 4E). Of the clones studied, $23.6\% \pm 12.5\%$ were holoclones, $34.9\% \pm 10.5\%$ were meroclones, and $41.5\% \pm 11.3\%$ were paraclones (Table 1). Our findings indicate that holoclone-, meroclone-, and paraclone-type cells, previously identified in skin and ocular surface, also comprise the proliferative compartment of the human oral mucosal epithelium.

To investigate the expression of p75 and integrin $\beta 1$ in these three clonal types, we performed immunohistochemical analysis and real-time PCR assay. Immunofluorescence showed that p75 was strongly expressed in the membrane of holoclone cells (Fig. 4G), moderately expressed in some of the small cells of meroclones (Fig. 4H), and not expressed in paraclone cells (Fig. 4I). In contrast, integrin $\beta 1$ was expressed in all three clonal types (Fig. 4J–4L). We used real-time PCR to assess p75 mRNA expression (supplemental online Fig. 2) and found that compared with meroclone and paraclone cells, in holoclone cells, mean p75 mRNA expression was significantly upregulated (*, $p < .05$, Mann-Whitney *U* test); all three clonal type cells

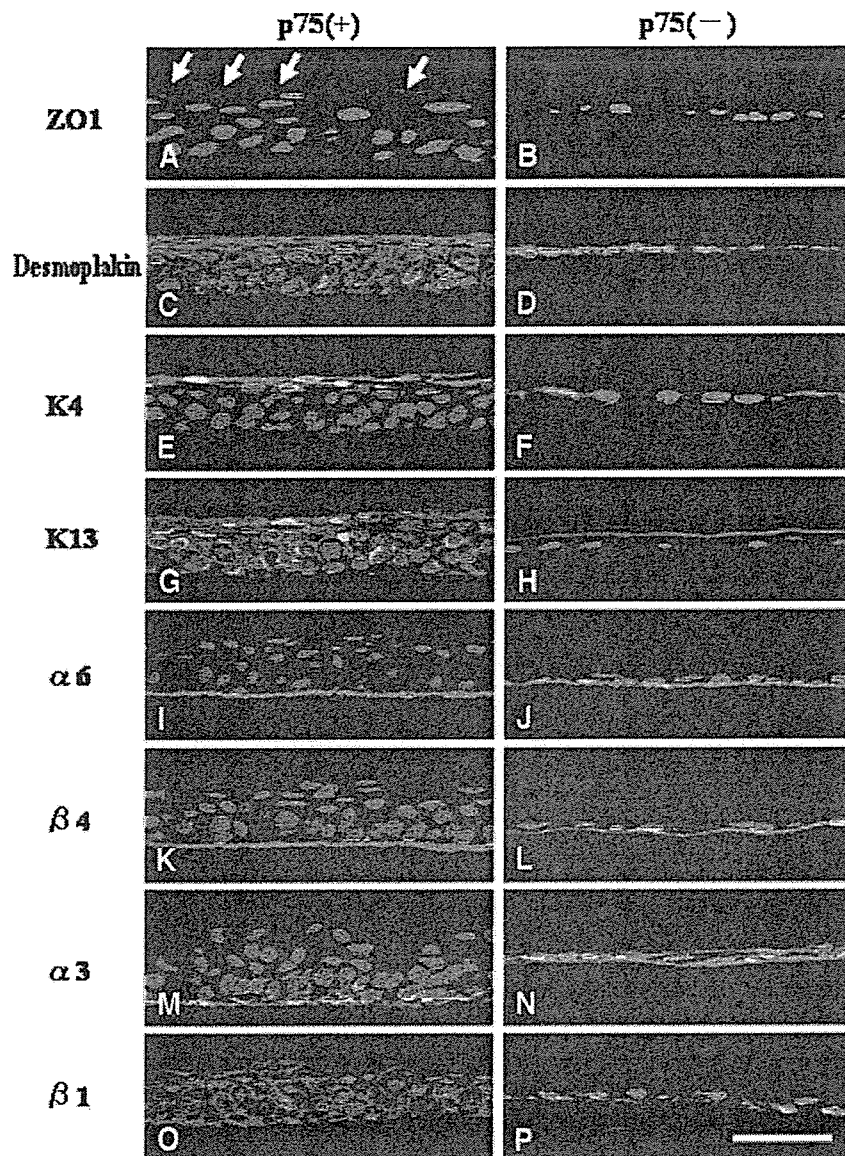


Figure 3. Representative immunofluorescence micrographs of p75(+) and p75(-) oral epithelial cells grown on amniotic membrane. ZO-1 was expressed on the apical surface of the p75(+) sheet but not the p75(-) sheet (A, B). Desmoplakin was clearly expressed in the cell membrane of the p75(+) sheet and moderately expressed in the p75(-) sheet (C, D). In the p75(+) sheet, mucosal-specific keratin 4 was expressed in the superficial portion and the upper half of the intermediate layers; keratin 13 was expressed in all epithelial layers except the basal cell layers (E, G). In the 75(-) sheet, there was no or faint superficial staining (F, H). The basement membrane assembly proteins integrin $\alpha 6/\beta 4$ showed linear positive staining on the basement membrane side of both p75(+) and p75(-) sheets (I-L). In both p75(+) and p75(-) sheets, integrin $\alpha 3$ was mainly expressed in the basal cell membrane (M, N). Integrin $\beta 1$ was expressed in the cell membrane of nearly all epithelial cells in the p75(+) sheet; only faint or moderate staining was observed in the p75(-) sheet (O, P). Scale bars = 100 μ m.

exhibited integrin $\beta 1$ mRNA expression. These findings showed that p75 was strongly expressed in holoclone-type cells, suggesting p75 as a potential marker for oral keratinocyte SC-containing populations.

The Role of Neurotrophin Signaling in p75(+) Oral Keratinocytes

To evaluate the role of neurotrophin/p75 signaling in cell growth, differentiation, and survival, we performed the BrdU ELISA cell proliferation assay, immunohistochemistry for differentiation markers (keratin 10 and 13), and UV-induced apoptosis assay (TUNEL) in the presence or absence of neurotrophins in an in vitro culture system. BrdU assay indicated that NGF and NT-3 stimulated p75(+) oral keratinocyte cell proliferation (Fig. 5; *, $p < .01$, t test). From our immunohistochemical results, there were no differences regarding the effect of neurotrophins on cell differentiation. All p75(+) cells incubated with neurotrophins showed the expression of mucosal-specific keratin 13 but not keratinization-specific keratin 10 (supplemental online Fig. 3). TUNEL assay indicated that neurotrophins

other than NGF fail to protect p75(+) oral keratinocytes from UV-induced apoptosis (Fig. 6). Our in vitro findings indicate that some neurotrophin/p75 signaling affects cell growth and survival but not cell differentiation.

DISCUSSION

The role of SCs in homeostasis, wound healing, and tumorigenesis and their identification and therapeutic use in tissue engineering, gene therapy, and the treatment of various diseases have gained attention. In view of ethical concerns surrounding the use of embryonic SCs, the identification of specific markers to isolate keratinocyte SC populations is of great value, both for a better understanding of SCs and for the development of SC-mediated regenerative therapies. We demonstrated the following points: (a) that p75(+) cell subsets are present as clusters in a specific region of the human oral mucosal epithelium and (b) that most of these cells do not cycle actively in vivo. Cell sorting showed that compared with p75(-) cells, p75(+) cells

Table 1. Classification of clonal types

Donor age/gender	Tissue origin	Original clone formation (%)	Each type of clone (%)		
			Holoclone	Meroclone	Paraclone
18/M	Buccal	16.7	16.7	33.3	50
29/F	Buccal	61	18.1	36.4	45.5
37/M	Buccal	75	16.7	50	33.3
44/M	Buccal	50	22.3	22.7	50
19/F	Gingiva	80.6	34.5	24.1	41.4
24/F	Gingiva	75	50	27.8	22.2
25/M	Gingiva	30.6	13.6	34.5	56.4
27/F	Gingiva	66.7	16.7	50	33.3
		56.9 ± 22.8	23.6 ± 12.5	34.9 ± 10.5	41.5 ± 11.3

Abbreviations: F, female; M, male.

(c) were smaller and (d) had higher *in vitro* proliferative capacity and clonal growth potential. Our single-cell clonal analysis revealed (e) that three clonal types, previously identified in skin and ocular surface, also comprise the proliferative compartment of human oral mucosal epithelium and (f) that p75 is strongly expressed in holoclones at both the mRNA and protein level. Our *in vivo* and *in vitro* findings indicate that p75 may represent a novel marker for oral keratinocyte SC-containing populations.

In this study, we demonstrate for the first time that human oral keratinocytes exhibit regional diversity with respect to p75 expression. In the buccal mucosa, p75 was mainly expressed in the tips of the papillae, whereas in gingiva it was observed in both the tips of the papillae and the deep rete ridges. In the current situation, we can not exactly determine whether this means there are two stem cell niches in gingiva. The precise location of stem/progenitor cells within the epithelium is a question that remains to be settled, and its proposed answer depends on the expression pattern, cell surface markers, specific tissues, and species. Others [12, 13] reported that SC distribution is nonrandom but varies by the specific phenotype of epithelial tissue. They found that cells brightly stained for integrin $\beta 1$, a putative epidermal SC marker, were located in the tips of dermal papillae in human foreskin and interfollicular scalp and in the deep rete ridges of the palm.

These cells, as was the case in our p75(+) cells, existed as clusters in tissue, rather than as sporadic single cells. Lavker and Sun [4, 7] studied the morphological and functional characteristics of epidermal SC located at different sites. Keratinocytes at the bottom of the rete ridges in foreskin and interfollicular scalp are protected, pigmented, and ultrastructurally primitive. They express less integrin $\beta 1$ than basal cells in the shallowest portion (tips of the papillae) of these areas of the epidermis. However, the latter tend to be more specialized ultrastructurally and are more vulnerable to environmental insults than basal cells located in the deep rete ridges. Our *in vivo* and *in vitro* findings indicate that p75 is a potential marker of oral keratinocytes in both stem and progenitor cells, so regarding the p75 expression pattern, we do not consider that there are two stem cell niches, but rather either the deep or shallow portion of the rete ridges are stem cell-containing compartments. We posit that from the recent reports using a cell surface marker for Dsg3 [39] and K15 [40], the location of stem and transient amplifying cells tends to be in the tips of the deep rete ridges. Additional cell biological studies are needed to clarify this point.

It is important to clarify how high p75 expression can better define human oral keratinocyte stem/progenitor cells compared with other previously reported epidermal keratinocyte SC phenotypes, such as integrin $\beta 1$ [12, 41], integrin $\alpha 6$ /CD71 [14, 15], and side population (SP) cells [42–45]. We also investigated the expression of CD34, a mouse bulge cell marker, and found that

like previous reports on human bulge cells [46–48], it was not expressed in any layer of human oral mucosal epithelium (data not shown). To elucidate the relationship between p75 and integrin $\beta 1$, integrin $\alpha 6$ /CD71, and SP, we investigated their expression level in all isolated p75(+) and p75(–) cell fractions using real-time PCR (supplemental online Fig. 4). Moreover, we have investigated the expression of these proposed epidermal SC markers and compared them with the expression of p75 in the serial cross sections using the appropriate mouse monoclonal antibodies (supplemental online Fig. 5). Real-time PCR showed that the level of integrin $\beta 1$ and ABCG2 mRNA in the p75(+) cell fraction was higher than that of the p75(–) cell fraction (supplemental online Fig. 4A, 4B; *, $p < .01$). Although there was some tendency toward a decreased CD71 mRNA level in p75(+) cell fractions, the level of both integrin $\alpha 6$ and CD71 mRNA was not statistically significant (supplemental online Fig. 4C, 4D). Immunohistochemical analysis showed that integrin $\beta 1$ was expressed in their basal and suprabasal cell layers (supplemental online Fig. 5B). The expression of p75 was observed in the restricted region of the basal cell layer (supplemental online Fig. 5A, 5C, 5F, *). Interestingly, immunohistochemistry showed that CD 71 was mainly expressed in the basal and suprabasal cells of human oral mucosal epithelium, and negative or low levels of CD71 cells were sporadically observed in the deep rete ridges (supplemental online Fig. 5D, *). Furthermore, BCRP1 was observed in the restricted region of the basal cells of human oral mucosal epithelium (supplemental online Fig. 5G, *). Based on these findings, the expression pattern of the proposed epidermal SC markers was partially overlapped but somewhat different from that of p75, suggesting that p75(+) oral keratinocytes may have different features from the proposed epidermal SC markers. However, these results alone do not allow us to fully explain the differences between p75 and proposed epidermal keratinocyte SC markers, and additional studies are under way in our laboratory to determine the precise character of p75(+) human oral keratinocytes.

Under steady-state conditions, SCs divide infrequently *in vivo* [49, 50]. However, they can proliferate vigorously *in vitro* and after appropriate stimulation *in vivo*. TACs, on the other hand, cycle actively. Cell kinetic studies, such as the label-retaining method, are clearly considered the gold standard by which to identify slow-cycling SCs. However, it is difficult to perform these kinds of cell kinetic studies in humans due to ethical considerations. Therefore, it is necessary to establish a useful assay to assign SC status isolated on the basis of biological markers in humans. In our study, most p75(+) basal cells did not express the proliferation-associated marker Ki67, suggesting that they did not cycle actively *in vivo*. Our finding that the human oral mucosal epithelium contained a small subset of p75(+)-Ki67(+) cells suggests that p75, although valuable for

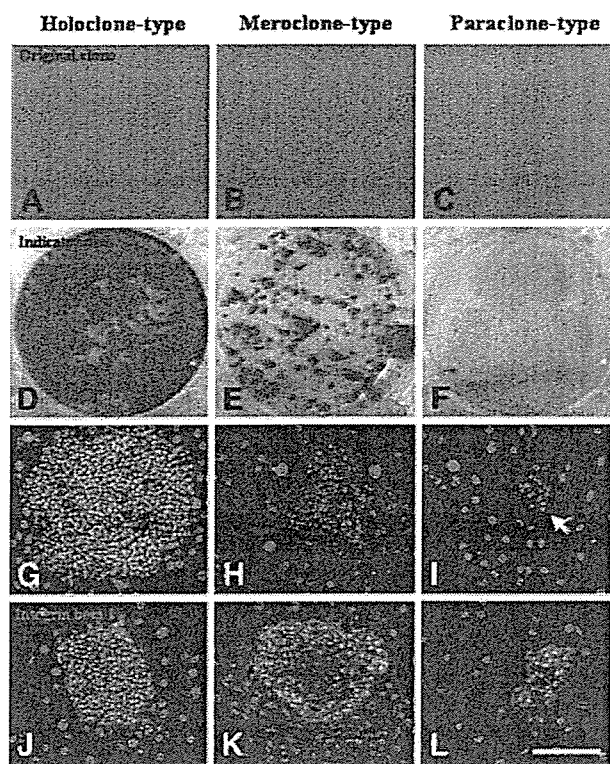


Figure 4. Isolation and clonal analysis of oral keratinocytes. The representative original clone of the holoclone type is large, has a relatively smooth perimeter, and contains mainly small cells (A). Most original clones of the paraclone type are small and contain large differentiated squamous cells (C). The meroclone type is intermediate between the holoclone and the paraclone (B). Toluidine blue staining (indicator dishes) clearly showed that the holoclone formed large, rapidly growing colonies, fewer than 5% of which aborted or differentiated terminally (D). The paraclone grew no colonies or only uniformly small terminal colonies (F). The meroclone formed growing and aborted colonies (E). Immunofluorescence showed that p75 was strongly expressed in the cell membrane of holoclone-type cells (G). In the meroclone-type cells, p75 was moderately expressed in some of the small cells (H). Paraclone-type cells did not express p75 (I). In contrast, integrin $\beta 1$ was expressed in the cell membrane of all three clonal types (J–L). Scale bars = 100 μm .

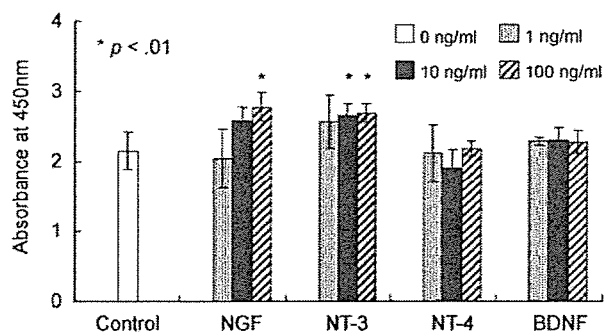


Figure 5. Neurotrophin effects on oral keratinocyte proliferation. 5-Bromo-2'-deoxyuridine (BrdU) enzyme-linked immunosorbent assay cell proliferation assay of p75 (+) oral epithelial cells cultivated in the presence (1, 10, and 100 ng/ml) and absence of neurotrophin (NGF, NT-3, NT-4, and BDNF)-supplemented media for 48 hours ($n = 5$). Scale bars indicate the mean values of BrdU absorbance in each culture condition. BrdU assay indicated that NGF and NT-3 stimulated p75(+) oral keratinocyte cell proliferation (*, $p < .01$, t test). Abbreviations: BDNF, brain-derived neurotrophic factor; NGF, nerve growth factor; NT, neurotrophin.

www.StemCells.com

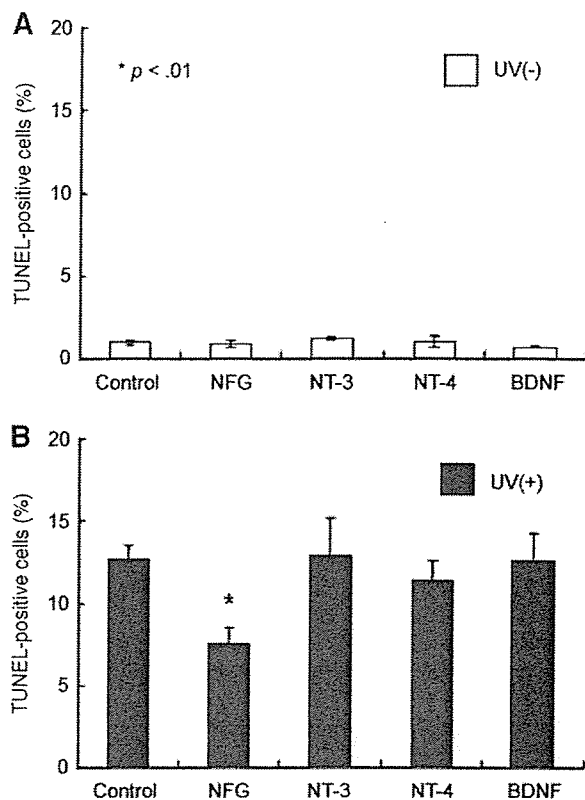


Figure 6. Neurotrophin effects on oral keratinocyte cell survival. The p75(+) oral epithelial cells were treated for 48 hours in the presence (100 ng/ml) and absence of neurotrophin (NGF, NT-3, NT-4, and BDNF)-supplemented media before, with, or without UV irradiation, and apoptosis was measured by TUNEL staining. The percentage of TUNEL(+) cells in each culture condition was calculated by three individual experiments. Without UV conditions, neurotrophins do not seem to influence cell death in these cells (A). Under UV(+) conditions, NGF exerts a protective effect against UV-induced apoptosis (*, $p < .01$, t test); however, the other neurotrophins do not prevent cell death (B). Abbreviations: BDNF, brain-derived neurotrophic factor; NGF, nerve growth factor; NT, neurotrophin; TUNEL, terminal deoxynucleotidyl transferase dUTP nick-end labeling.

sorting SC populations, may also identify early TAC populations on the basis of their cell-cycling status.

Others reported that cell size may distinguish SCs from TACs or differentiated cells. In the epidermis, the response to phorbol esters of the smallest keratinocytes is different from that of other cells [51, 52]. These keratinocytes also exhibited the highest clonogenicity; cultured keratinocytes isolated from human epidermis formed clones when they were 11 μm or less in diameter, and they terminally differentiated when they were 12 μm or more in diameter [29]. The average diameter of our p75(+) cells was $11.4 \pm 3.8 \mu\text{m}$, which is consistent with the report of Barrandon and Green [29]. Based on these findings and on the reported size of corneal epithelial SCs [53], we suggest that cell size is a potential indicator of keratinocyte SCs, not only of the epidermis, but also of other epithelial cell types.

We found that isolated keratinocytes fractionated on the basis of the intensity of their p75 expression could produce different cell populations with different properties. Only cells in the p75(+) population exhibited exceptionally high proliferative potential, CFE, and 3D tissue forming-ability, features associated with SC populations and consistent with esophageal keratinocyte SCs studied *in vitro* [28]. However, SC-rich fractions from adult rat epidermis [54] and neonatal human foreskin [55]

manifested substantially lower CFE than the source populations. Moreover, in standard tissue cultures, exhaustion of the proliferative potential of keratinocytes can be slowed by amending the culture conditions [56]. These discrepancies may be related to species differences (human and rodent), the cell isolation techniques used, and the biological state of the keratinocyte SCs in culture. Although the cell-sorting procedure using specific cell-surface markers is useful [12, 55], the isolated cells are released from the control mechanisms regulating the *in vivo* SC niche that renders them slow-cycling.

Although cultured human keratinocytes may not retain all their *in vivo* characteristics after removal from their microenvironment, they are clonogenic [12, 13, 49] and able to generate three distinct clonal forms due to the varied self-renewal capacities of individual keratinocytes [9]. Analysis of clonal-type frequency after a period of *in vitro* growth yields information on the intrinsic nature and proliferative potential of the original keratinocyte populations. The three clonal types we identified (holoclone, meroclone, and paraclone) comprise the proliferative compartment of the human oral mucosal epithelium. As p75 was intensively expressed only by holoclone cells on both the mRNA and protein level, it may specifically characterize human oral keratinocyte SC-containing population.

In contrast, integrin $\beta 1$, an epidermal SC marker, was expressed in all three clonal-type cells. According to De Luca et al. [57] and Nguyen et al. [58], keratinocyte SCs completely disappeared in most mitogenic tissue culture environments and exhibited marked changes in their expression of integrin and other markers. Cell-surface receptor molecules are particularly useful for isolating SC compartments; however, reliance on cell adhesion molecules alone may be inadequate for SC isolation because almost all basal keratinocytes express these molecules, which are essential for biological processes, to various degrees [14, 59–61]. Therefore, markers specific for *in vivo* keratinocyte SCs may differ from those of keratinocyte colonies grown *in vitro*.

We also posit that it is very important to carefully interpret the results of stem cell research. Our conclusion that p75 may represent a marker for a human oral keratinocyte stem cell-containing population was mainly based on the results obtained by short-term *in vitro* clonogenic assay and tissue-regenerative ability, not by *in vivo* long-term reconstitution assay [62–64]. We truly recognize that sustained epithelial tissue regeneration in an appropriate *in vivo* transplant model is likely to be the best functional definition of keratinocyte stem cells. Even though *in vitro* assay with development of culture techniques for keratinocytes is believed to reflect the extensive capacity expected of keratinocyte stem cells *in vivo*, at present our *in vitro* assay alone does not allow us to fully characterize the human oral keratinocyte stem cells. Even though it is quite difficult to transplant human oral keratinocytes onto the oral cavity site, both technically and methodologically, an additional *in vivo* long-term assay is needed to clarify these points.

In several cell types, the protein family of mammalian neurotrophins (NGF, BDNF, and NT-3/4/5) supports cell survival, differentiation, and plasticity [65, 66]. The elucidation of the role of neurotrophin/p75 signaling in oral keratinocyte stem cells is important for better understanding the mechanism of stem cell behavior. In our series, one of the representative

neurotrophin molecules, “NGF,” can support keratinocyte cell proliferation and protect the cells from apoptosis. These results were consistent with the previous reports using other cell types [31, 66–72]. We also pointed out that effects of neurotrophins are mediated via the activation of two different classes of plasma membrane receptor, high-affinity Trk tyrosine kinase receptors (TrkA, TrkB, and TrkC) and low-affinity p75 neurotrophin receptors that form complexes. For example, p75 modulates cell death in different models [73–75]. Proapoptotic signaling occurs when p75 is expressed alone without the coexpression of Trk receptors [76, 77]. Thus, the cell death-inducing or cell-survival actions of neurotrophins are strongly dependent on the relative expression of p75 and Trk receptors on the target-cell populations. Studies are under way to elucidate the relationship between p75 and Trk receptors in keratinocytes from human oral mucosal tissue.

We believe that one way to characterize distinct cell populations is to generate global gene expression profiles. Recently, several microarray profiles of mouse [37, 78] and human [46] hair follicle bulge cells were reported. In these results, upregulation of p75 has not been identified in the bulge cells, yet we consider that oral mucosal epithelium is fundamentally different from bulge cells and epidermis, which may explain why upregulation of p75 was not detected. Moreover, the data represent the average characteristics of a cell population, rather than the properties of individual cells.

Our study showed that oral keratinocytes expressing the p75(+) phenotype exhibited properties suggesting that they are equivalent to the SC-containing population. The degree of SC sorting made possible by p75 will allow the further fractionation and analysis of SC populations, thereby facilitating the identification of a set of additional SC markers unique to the epithelium. Systematic evaluation using cell-sorting techniques and clonal analysis will facilitate the identification and purification of these cells and greatly contribute to our understanding of SC biology. In addition, greater knowledge regarding SCs will provide a foundation for the development of treatments for epithelium-related diseases.

ACKNOWLEDGMENTS

We thank Yann Barrandon for advising the clonal analysis system, Narisato Kanamura and Takashi Amemiya for performing the oral biopsies, Hideo Honjyo for providing AM, and Hisayo Sogabe and Tomoko Horikiri for assisting with the culture procedures. This study was supported in part by Grants-in-Aid for Scientific Research from the Japanese Ministry of Health, Labor and Welfare (H16-Saisei-007) and by the Japanese Ministry of Education, Culture, Sports, Science and Technology (Kobe Translational Research Cluster), a research grant from the Kyoto Foundation for the Promotion of Medical Science, and the Intramural Research Fund of Kyoto Prefectural University of Medicine.

DISCLOSURES

The authors indicate no potential conflicts of interest.

REFERENCES

1 Watt FM. Terminal differentiation of epidermal keratinocytes. *Curr Opin Cell Biol* 1989;1:1107–1115.

2 Lajtha LG. Stem cell concepts. *Differentiation* 1979;14:23–34.
3 Leblond CP. The life history of cells in renewing systems. *Am J Anat* 1981;160:114–158.
4 Lavker RM, Sun TT. Heterogeneity in epidermal basal keratinocytes: Morphological and functional correlations. *Science* 1982;215:1239–1241.

- 5 Hall PA, Watt FM. Stem cells: The generation and maintenance of cellular diversity. *Development* 1989;106:619–633.
- 6 Potten CS, Loeffler M. Stem cells: Attributes, cycles, spirals, pitfalls and uncertainties. Lessons for and from the crypt. *Development* 1990;110:1001–1020.
- 7 Lavker RM, Sun TT. Epidermal stem cells. *J Invest Dermatol* 1983;81:121s–127s.
- 8 Reid LM. Stem cell-fed maturational lineages and gradients in signals: Relevance to differentiation of epithelia. *Mol Biol Rep* 1996;23:21–33.
- 9 Barrandon Y, Green H. Three clonal types of keratinocyte with different capacities for multiplication. *Proc Natl Acad Sci U S A* 1987;84:2302–2306.
- 10 Rochat A, Kobayashi K, Barrandon Y. Location of stem cells of human hair follicles by clonal analysis. *Cell* 1994;76:1063–1073.
- 11 Pellegrini G, Gofisano O, Paterna P et al. Location and clonal analysis of stem cells and their differentiated progeny in the human ocular surface. *J Cell Biol* 1999;145:769–782.
- 12 Jones PH, Watt FM. Separation of human epidermal stem cells from transit amplifying cells on the basis of differences in integrin function and expression. *Cell* 1993;73:713–724.
- 13 Jones PH, Harper S, Watt FM. Stem cell patterning and fate in human epidermis. *Cell* 1995;80:83–93.
- 14 Tani H, Morris RJ, Kaur P. Enrichment for murine keratinocyte stem cells based on cell surface phenotype. *Proc Natl Acad Sci U S A* 2000;97:10960–10965.
- 15 Li A, Pouliot N, Redvers R et al. Extensive tissue-regenerative capacity of neonatal human keratinocyte stem cells and their progeny. *J Clin Invest* 2004;113:390–400.
- 16 De Luca M, Albanese E, Megna M et al. Evidence that human oral epithelium reconstituted in vitro and transplanted onto patients with defects in the oral mucosa retains properties of the original donor site. *Transplantation* 1990;50:454–459.
- 17 Hata K, Ueda M. Fabrication of cultured epithelium using oral mucosal cells and its clinical applications. *Hum Cell* 1996;9:91–96.
- 18 Nakamura T, Endo K, Cooper LJ et al. The successful culture and autologous transplantation of rabbit oral mucosal epithelial cells on amniotic membrane. *Invest Ophthalmol Vis Sci* 2003;44:106–116.
- 19 Nakamura T, Inatomi T, Sotozono C et al. Transplantation of cultivated autologous oral mucosal epithelial cells in patients with severe ocular surface disorders. *Br J Ophthalmol* 2004;88:1280–1284.
- 20 Nakamura T, Ang LP, Rigby H et al. The use of autologous serum in the development of corneal and oral epithelial equivalents in patients with Stevens Johnson syndrome. *Invest Ophthalmol Vis Sci* 2006;47:909–916.
- 21 Nishida K, Yamato M, Hayashida Y et al. Corneal reconstruction with tissue-engineered cell sheets composed of autologous oral mucosal epithelium. *N Engl J Med* 2004;351:1187–1196.
- 22 Pellegrini G. Changing the cell source in cell therapy? *N Engl J Med* 2004;351:1170–1172.
- 23 Inatomi T, Nakamura T, Koizumi N et al. The mid-term results of ocular surface reconstruction using cultivated autologous oral mucosal epithelial transplantation. *Am J Ophthalmol* 2006;141:267–275.
- 24 Rodriguez-Tebar A, Dechant G, Gotz R et al. Binding of neurotrophin-3 to its neuronal receptors and interactions with nerve growth factor and brain-derived neurotrophic factor. *EMBO J* 1992;11:917–922.
- 25 Smith CA, Farrah T, Goodwin RG. The TNF receptor superfamily of cellular and viral proteins: Activation, costimulation, and death. *Cell* 1994;76:959–962.
- 26 Dechant G, Barde YA. Signalling through the neurotrophin receptor p75^{NTR}. *Curr Opin Neurobiol* 1997;7:413–418.
- 27 Botchkarev VA, Botchkareva NV, Albers KM et al. A role for p75 neurotrophin receptor in the control of apoptosis-driven hair follicle regression. *FASEB J* 2000;13:1931–1942.
- 28 Okumura T, Shimada Y, Imamura M et al. Neurotrophin receptor p75^(NTR) characterizes human esophageal keratinocyte stem cells in vitro. *Oncogene* 2003;22:4017–4026.
- 29 Barrandon Y, Green H. Cell size as a determinant of the clone-forming ability of human keratinocytes. *Proc Natl Acad Sci U S A* 1985;82:5390–5394.
- 30 Ang LP, Tan DT, Beuerman RW et al. Development of a conjunctival epithelial equivalent with improved proliferative properties using a multistep serum-free culture system. *Invest Ophthalmol Vis Sci* 2004;45:1789–1795.
- 31 Marconi A, Vaschieri C, Zanoli S et al. Nerve growth factor protects human keratinocytes from ultraviolet-B-induced apoptosis. *J Invest Dermatol* 1999;113:920–927.
- 32 Bickelbach JR. Identification and behavior of label-retaining cells in oral mucosa and skin. *J Dent Res* 1981;60:1611–1620.
- 33 Cotsarelis G, Cheng SZ, Dong G et al. Existence of slow-cycling limbal epithelial basal cells that can be preferentially stimulated to proliferate: Implications on epithelial stem cells. *Cell* 1989;57:201–209.
- 34 Fortunel N, Batard P, Hatzfeld A et al. High proliferative potential-quietest cells: A working model to study primitive quiescent hematopoietic cells. *J Cell Sci* 1998;111:1867–1875.
- 35 Lehrer MS, Sun TT, Lavker RM. Strategies of epithelial repair: Modulation of stem cell and transit amplifying cell proliferation. *J Cell Sci* 1998;111:2867–2875.
- 36 Braun KM, Niemann C, Jensen UB et al. Manipulation of stem cell proliferation and lineage commitment: Visualisation of label-retaining cells in whole mounts of mouse epidermis. *Development* 2003;130:5241–5255.
- 37 Tumber T, Guasch G, Greco V et al. Defining the epithelial stem cell niche in skin. *Science* 2004;303:359–363.
- 38 Mather MB, Ferrari G, Dellambra E et al. Clonal analysis of stably transduced human epidermal stem cells in culture. *Proc Natl Acad Sci U S A* 1996;93:10371–10376.
- 39 Wan H, Stone MG, Simpson C et al. Desmosomal proteins, including desmoglein 3, serve as novel negative markers for epidermal stem cell-containing population of keratinocytes. *J Cell Sci* 2003;116:4239–4248.
- 40 Webb A, Li A, Kaur P. Location and phenotype of human adult keratinocyte stem cells of the skin. *Differentiation* 2004;72:387–395.
- 41 Blanpain C, Lowry WE, Geoghegan A et al. Self-renewal, multipotency, and the existence of two cell populations within an epithelial stem cell niche. *Cell* 2004;118:635–648.
- 42 Terunuma A, Jackson KL, Kapoor V et al. Side population keratinocytes resembling bone marrow side population stem cells are distinct from label-retaining keratinocyte stem cells. *J Invest Dermatol* 2003;121:1095–1103.
- 43 Triel C, Vestergaard ME, Bolund L et al. Side population cells in human and mouse epidermis lack stem cell characteristics. *Exp Cell Res* 2004;295:79–90.
- 44 Yano S, Ito Y, Fujimoto M et al. Characterization and localization of side population cells in mouse skin. *STEM CELLS* 2005;23:834–841.
- 45 Redvers RP, Li A, Kaur P. Side population in adult murine epidermis exhibits phenotypic and functional characteristics of keratinocyte stem cells. *Proc Natl Acad Sci U S A* 2006;103:13168–13173.
- 46 Ohyama M, Terunuma A, Teck CL et al. Characterization and isolation of stem cell-enriched human hair follicle bulge cells. *J Clin Invest* 2006;116:249–260.
- 47 Cotsarelis G. Gene expression profiling gets to the root of human hair follicle stem cells. *J Clin Invest* 2006;116:19–22.
- 48 Cotsarelis G. Epithelial stem cells: A folliculocentric view. *J Invest Dermatol* 2006;126:1459–1468.
- 49 Potten CS, Morris RJ. Epithelial stem cells in vivo. *J Cell Sci* 1988;10:45–62.
- 50 Cotsarelis G, Sun TT, Lavker RM. Label-retaining cells reside in the bulge area of pilosebaceous unit: Implications for follicular stem cells, hair cycle, and skin carcinogenesis. *Cell* 1990;61:1329–1337.
- 51 Furstenberger G, Gross M, Schweizer J et al. Isolation, characterization and in vitro cultivation of subfractions of neonatal mouse keratinocytes: Effects of phorbol esters. *Carcinogenesis* 1986;7:1745–1753.
- 52 Gross M, Furstenberger G, Marks F. Isolation, characterization, and in vitro cultivation of keratinocyte subfractions from adult NMRI mouse epidermis: Epidermal target cells for phorbol esters. *Exp Cell Res* 1987;171:460–474.
- 53 Romano AC, Espana EM, Yoo SH et al. Different cell sizes in human limbal and central corneal basal epithelia measured by confocal microscopy and flow cytometry. *Invest Ophthalmol Vis Sci* 2003;44:5125–5129.
- 54 Pavlovitch JH, Rizk-Rabin M, Jaffray P et al. Characteristics of homogeneously small keratinocytes from newborn rat skin: Possible epidermal stem cells. *Am J Physiol* 1991;261:C964–C972.
- 55 Li A, Simmons PJ, Kaur P. Identification and isolation of candidate human keratinocyte stem cells based on cell surface phenotype. *Proc Natl Acad Sci U S A* 1998;95:3902–3907.
- 56 Rheinwald JG, Green H. Epidermal growth factor and the multiplication of cultured human epidermal keratinocytes. *Nature* 1977;265:421–424.
- 57 De Luca M, Pellegrini G, Bondanza S et al. The control of polarized integrin topography and the organization of adhesion-related cytoskeleton in normal human keratinocytes depend upon number of passages in culture and ionic environment. *Exp Cell Res* 1992;202:142–150.
- 58 Nguyen BP, Ryan MC, Gil SG et al. Deposition of laminin 5 in epidermal wounds regulates integrin signaling and adhesion. *Curr Opin Cell Biol* 2000;12:554–562.
- 59 Peltonen J, Larjava H, Jaakkola S et al. Localization of integrin receptors for fibronectin, collagen, and laminin in human skin. Variable expression in basal and squamous cell carcinomas. *J Clin Invest* 1989;84:1916–1923.
- 60 Carter WG, Wayner EA, Bouchard TS et al. The role of integrins alpha 2 beta 1 and alpha 3 beta 1 in cell-cell and cell-substrate adhesion of human epidermal cells. *J Cell Biol* 1990;110:1387–1404.
- 61 Dowling J, Yu QC, Fuchs E. Beta4 integrin is required for hemidesmosome formation, cell adhesion and cell survival. *J Cell Biol* 1996;134:559–572.
- 62 Kolodka TM, Garlick JA, Taichman LB. Evidence for keratinocyte stem cells in vitro: Long term engraftment and persistence of transgene expression from retrovirus-transduced keratinocytes. *Proc Natl Acad Sci U S A* 1998;95:4356–4361.
- 63 Schneider TE, Barland C, Alex AM et al. Measuring stem cell frequency

- in epidermis: A quantitative in vivo functional assay for long-term repopulating cells. *Proc Natl Acad Sci U S A* 2003;100:11412–11417.
- 64 Pouliot N, Redvers RP, Ellis S et al. Optimization of a transplant model to assess skin reconstitution from stem cell-enriched primary human keratinocyte populations. *Exp Dermatol* 2005;14:60–69.
- 65 Poo MM. Neurotrophins as synaptic modulators. *Nat Rev Neurosci* 2001;2:24–32.
- 66 Botchkarev VA, Yaar M, Peters EM et al. Neurotrophins in skin biology and pathology. *J Invest Dermatol* 2006;126:1719–1727.
- 67 Matsuda H, Coughlin MD, Bienenstock J et al. Nerve growth factor promotes human hemopoietic colony growth and differentiation. *Proc Natl Acad Sci U S A* 1988;85:6508–6512.
- 68 Kannan Y, Ushio H, Koyama H et al. 2.5S nerve growth factor enhances survival, phagocytosis, and superoxide production of murine neutrophils. *Blood* 1991;77:1320–1325.
- 69 Paus R, Lufil M, Czarnetzki BM. Nerve growth factor modulates keratinocyte proliferation in murine skin organ culture. *Br J Dermatol* 1994;130:174–180.
- 70 Di Marco E, Mather M, Bondanza S et al. Nerve growth factor binds to normal human keratinocytes through high and low affinity receptors and stimulates their growth by a novel autocrine loop. *J Biol Chem* 1993;268:22838–22846.
- 71 Touhami A, Grueterich M, Tseng SC. The role of NGF signaling in human limbal epithelium expanded by amniotic membrane culture. *Invest Ophthalmol Vis Sci* 2002;43:987–994.
- 72 Marcomi A, Terracina M, Fila C et al. Expression and function of neurotrophins and their receptors in cultured human keratinocytes. *J Invest Dermatol* 2003;121:1515–1521.
- 73 Carter BD, Kaltschmidt C, Kaltschmidt B et al. Selective activation of NF-kappa B by nerve growth factor through the neurotrophin receptor p75. *Science* 1996;272:542–545.
- 74 Frade JM, Rodriguez-Tebar A, Barde YA. Induction of cell death by endogenous nerve growth factor through its p75 receptor. *Nature* 1996;383:166–168.
- 75 Yaar M, Zhai S, Pilch PF et al. Binding of beta-amyloid to the p75 neurotrophin receptor induces apoptosis. A possible mechanism for Alzheimer's disease. *J Clin Invest* 1997;100:2333–2340.
- 76 Carter BD, Lewin GR. Neurotrophins live or let die: Does p75NTR decide? *Neuron* 1997;18:187–190.
- 77 Yoon SO, Casaccia-Bonnel P, Carter B et al. Competitive signaling between TrkA and p75 nerve growth factor receptors determines cell survival. *J Neurosci* 1998;18:3273–3281.
- 78 Morris RJ, Liu Y, Marles L et al. Capturing and profiling adult hair follicle stem cells. *Nat Biotechnol* 2004;22:411–417.



See www.StemCells.com for supplemental material available online.

The Use of Autologous Serum in the Development of Corneal and Oral Epithelial Equivalents in Patients with Stevens-Johnson Syndrome

Takahiro Nakamura,^{1,2} Leonard P. K. Ang,^{1,3} Helen Rigby,⁴ Eiichi Sekiyama,¹ Tsutomu Inatomi,¹ Chie Sotozono,¹ Nigel J. Fullwood,³ and Shigeru Kinoshita¹

PURPOSE. To evaluate the use of autologous serum (AS) from patients with severe ocular surface disease (OSD) in the development of transplantable corneal and oral epithelial tissue equivalents and to compare it with the use of conventional culture methods by using fetal bovine serum (FBS).

METHODS. AS was obtained from patients with severe OSD secondary to Stevens-Johnson syndrome. Corneal and oral epithelial cells were cultivated in medium supplemented with either AS or FBS. Corneal and oral epithelial equivalents were constructed on denuded amniotic membranes. The bromodeoxyuridine (BrdU) ELISA cell proliferation assay and colony-forming efficiency (CFE) of cells cultivated in AS- or FBS-supplemented media were compared. The morphologic characteristics and the basement membrane assembly of cultivated epithelial equivalents were analyzed by light and electron microscopy, as well as by immunohistochemistry.

RESULTS. BrdU proliferation assay and CFE analysis showed that human corneal and oral epithelial cells cultivated in AS-supplemented media had comparable proliferative capacities compared with FBS-supplemented media. The corneal and oral epithelial equivalents cultivated in AS- and FBS-supplemented media were morphologically similar and demonstrated the normal expression of tissue-specific keratins and basement membrane assembly. The presence of a well-formed stratified epithelium, a basement membrane, and hemidesmosomal attachments was confirmed by electron microscopy.

CONCLUSIONS. AS-supplemented cultures were effective in supporting the proliferation of human corneal and oral epithelial cells, as well as the development of transplantable epithelial equivalents. The use of AS is of clinical importance in the development of autologous xenobiotic-free bioengineered oc-

ular surface equivalents for clinical transplantation. (*Invest Ophthalmol Vis Sci.* 2006;47:909–916) DOI:10.1167/iovs.05-1188

Severe ocular surface disease (OSD), arising from conditions such as Stevens-Johnson syndrome (SJS) and ocular cicatricial pemphigoid, is a potentially devastating condition with significant visual morbidity. In such cases, the corneal epithelial stem cells in the limbus are destroyed, resulting in invasion of the corneal surface by surrounding conjunctiva, neovascularization, chronic inflammation, ingrowth of fibrous tissue, and stromal scarring.^{1–3} Conventional corneal transplantation in these patients is associated with dismal results. Alternative methods such as keratoepithelioplasty and limbal transplantation have been used to reconstruct these severely damaged eyes, with improved clinical outcomes.^{4,5} More recently, cultivated corneal epithelial stem cell transplantation has demonstrated promising results and has gained general acceptance as an effective treatment modality.^{6–9} We,¹⁰ together with other investigators,¹¹ have also demonstrated the effective use of autologous cultivated oral epithelial transplantation for the treatment of severe OSD, with the advantage that this reduces the risk of allograft rejection and the need for long-term steroids or immunosuppression.

The currently preferred method of cultivating corneal or oral epithelial cells requires the use of xenobiotic materials, such as fetal bovine serum (FBS) and 3T3 feeder cells, in the culture system. Various serum-free culture systems, developed to obviate the need for FBS, have mainly been used to study the roles of various growth factors.^{12–14} The clinical use of these serum-free culture systems has been limited because of their lower efficacy for cell propagation compared with bovine serum-supplemented medium. In the development of tissue equivalents for clinical transplantation, the ideal culture condition is one that is safe from disease transmission, as well as being able to support cell proliferation and differentiation. The use of autologous human serum as an alternative to FBS is therefore significantly advantageous, because it eliminates the need for bovine material in the culture process. This is particularly important when *ex vivo* expanding cells for clinical transplantation, because it reduces the risk of transmission of diseases, for example, spongiform encephalitis, or other unknown infections.

Ang et al.¹⁵ previously showed that human serum was able to support the *in vitro* and *in vivo* proliferation of cultivated human conjunctival cells. We wanted to determine whether autologous serum (AS) from patients with severe OSD was similarly efficacious in supporting cell proliferation, as well as the development of cultivated ocular surface epithelial equivalents, compared with conventional FBS supplemented culture conditions. We also sought to show that these transplantable bioengineered epithelial equivalents bore similar morphologic characteristics and differentiation-related keratin expression as the tissue of origin and possessed the necessary cell-to-cell and cell-to-substrate junctional elements (such as integrins and hemidesmosomes) for ensuring graft integrity after transplan-

From the ¹Department of Ophthalmology, Kyoto Prefectural University of Medicine, Graduate School of Medicine, Kyoto, Japan; ²Research Center for Regenerative Medicine, Doshisha University, Kyoto, Japan; ³Singapore National Eye Center, Singapore; and ⁴Institute of Environmental and Natural Sciences, Lancaster University, Lancaster, United Kingdom.

Supported in part by Grants-in-Aid for scientific research from the Japanese Ministry of Education, Culture, Sports, Science and Technology; a research grant from the Kyoto Foundation for the Promotion of Medical Science; and the Intramural Research Fund of Kyoto Prefectural University of Medicine.

Submitted for publication September 6, 2005; revised October 27, 2005; accepted January 11, 2006.

Disclosure: T. Nakamura, None; L.P.K. Ang, None; H. Rigby, None; E. Sekiyama, None; T. Inatomi, None; C. Sotozono, None; N.J. Fullwood, None; S. Kinoshita, None

The publication costs of this article were defrayed in part by page charge payment. This article must therefore be marked "advertisement" in accordance with 18 U.S.C. §1734 solely to indicate this fact.

Corresponding author: Takahiro Nakamura, Department of Ophthalmology, Kyoto Prefectural University of Medicine, Kawaramachi Hirokoji, Kamigyo-ku, Kyoto 602-0841, Japan; tnakamur@ophth.kpu-m.ac.jp.

tation. To our knowledge, a study of this nature has not been previously reported. This study has important clinical implications, because it provides the basis for developing safer autologous bioengineered tissues for clinical transplantation.

MATERIALS AND METHODS

All experimental procedures and clinical applications introduced here were approved by the Institutional Review Board for Human Studies of Kyoto Prefectural University of Medicine; prior informed consent was obtained from all patients in accordance with the tenets of the Declaration of Helsinki for research involving human subjects.

Preparation of Amniotic Membrane

Human amniotic membranes (AM) were obtained from mothers who had undergone cesarean sections. Under sterile conditions, the membranes were washed with PBS that contained antibiotics (5 mL 0.5% levofloxacin) and were stored at -80°C in modified medium (Dulbecco's modified Eagle's medium; GibcoBRL, Rockville, MD) and glycerol (Wako Pure Chemical Industries, Osaka, Japan) in the ratio of 1:1 by volume. Immediately before use, the AM was thawed, washed three times with sterile PBS that contained antibiotics, and cut into pieces approximately 4×4 cm in size. The overlying amniotic epithelial cells were removed by incubation with 0.02% EDTA (Nacalai Tesque Co., Kyoto, Japan) at 37°C for 2 hours, followed by gentle scraping with a cell scraper (Nunc International, Naperville, IL).

Subjects and Harvesting of Serum

Patients with severe OSD secondary to SJS were enrolled in the study. These patients manifested severe destruction of the ocular surface, limbal stem cell deficiency, total conjunctivalization of the cornea, and conjunctival cicatrization. The patients comprised 1 male and 3 females; their ages ranged from 27 to 69 years (mean, 49.3 ± 22.4 years). AS was obtained from these patients. Venesection was performed at the antecubital fossa under aseptic conditions; 30 mL of blood was collected into a sterile container, centrifuged, and filtered; the resultant serum (approximately 10 mL) was purified. Each patient's serum was stored in sterile tubes at -30°C . For experimental controls, we used 4 randomly selected distinct lots of FBS (ICN Inc., Aurora, OH).

Cultivation of Human Corneal and Oral Epithelial Cells

Corneal Epithelial Culture. Because all these patients had bilateral limbal stem cell deficiency, with the absence of any normal corneal epithelium, corneal epithelial cells were obtained from human corneoscleral rims from the Northwest Lion Eye Bank (Seattle, WA). These corneoscleral rims were first incubated at 37°C for 1 hour with 1.2 IU dispase to separate the epithelial cells, as previously described.¹⁶ Cells from the limbal and peripheral corneal region were carefully separated from the underlying stroma.

Oral Epithelial Culture. We obtained oral mucosal biopsy specimens ($2-3 \text{ mm}^2$) from these patients and volunteers while they were under local anesthesia. The submucosal connective tissue was removed with scissors to the extent possible; the resulting samples were then incubated at 37°C for 1 hour with 1.2 IU dispase, as previously described,¹⁷ and were treated with 0.05% Trypsin-EDTA solution for 10 minutes at room temperature to separate the cells.

After cell separation, the resultant corneal and oral epithelial cells were then seeded onto tissue culture dishes at a density of 1×10^4 cells/cm². The culture medium consisted of defined keratinocyte growth medium (KGM; Amniotec, Tokyo, Japan) supplemented with

5% AS or 5% FBS, as well as insulin (5 $\mu\text{g}/\text{mL}$), cholera toxin (0.1 nmol/L), human-recombinant epidermal growth factor (10 ng/mL), and penicillin-streptomycin (50 IU/mL).¹⁸ Cultures were incubated at 37°C in a 5% CO₂-95% air incubator, and the medium was changed every day.

Quantitation of Proliferative Capacity and Clonal Growth of Cells

The following proliferation assays were used to assess the proliferative capacity of the cells cultured with either AS- or FBS-supplemented media.

Bromodeoxyuridine (BrdU)-ELISA Cell Proliferation Assay. The proliferative capacity of human corneal or oral epithelial cells (passage 1) was determined by a BrdU-ELISA cell proliferation assay (Amersham Biosciences, Freiburg, Germany) by using a previously reported protocol.^{15,19} Analyses were performed on the sixth day of passage. Cultured cells were incubated with 10 μM BrdU-labeling solution for 20 hours at 37°C , followed by washing with 250 μL PBS that contained 10% serum per well. They were fixed with 70% ethanol in hydrochloric acid for 30 minutes at -20°C and incubated with 100 μL of monoclonal antibody against BrdU for 90 minutes, followed by 100 μL peroxidase substrate per well. The BrdU absorbance in each well was measured directly with a spectrophotometric microplate reader at a test wavelength of 450 nm and a reference wavelength of 490 nm. This gave us a measure of the degree of cell proliferation, which we termed the proliferation index (PI). Each sample was cultured in triplicate.

Colony-forming Efficiency. The clonal growth ability of cultured corneal or oral epithelial cells by using AS- and FBS-supplemented media was determined by the colony-forming efficiency (CFE). Cells were plated at a clonal density of 1000 cells onto 6-well culture dishes. A colony was defined as a group of eight or more contiguous cells.^{15,19} The colonies were fixed on day 8, stained with 0.1% Truidine blue and counted independently by 3 investigators; the data were then averaged. Each sample was cultured in triplicate.

The CFE was defined as follows

$$\text{CFE (\%)} = \frac{\text{Colonies formed at the end of growth period}}{\text{Total number of viable cells seeded}} \times 100 (\%)$$

The Development of Corneal and Oral Epithelial Equivalents

Corneal and oral epithelial cells were initially enzymatically separated as described above. The separated cells were then seeded onto denuded amniotic membranes spread on culture inserts in 6-well culture plates, at a density of 1×10^5 cells/well. These were cocultured with mitomycin-C-inactivated 3T3 fibroblasts (2×10^4 cells/cm²).^{17,18} The cells were incubated with AS- and FBS-supplemented culture media, as described above. The cultures were submerged in medium for 2 weeks and then exposed to air by lowering the medium level (airlifting) for 1 to 2 days. Cultures were incubated at 37°C in a 5% CO₂-95% air incubator, and the medium was changed every day.

Immunohistochemistry

Immunohistochemical studies of several tissue-specific keratins and basement membrane-related proteins in corneal and oral epithelial sheets cultivated by using AS- or FBS-supplemented media were carried out by following our previously described method.^{20,21} Normal human cornea and oral samples were also examined for comparison. Briefly, cryostat sections (7- μm thick) were placed on gelatin-coated slides and air-dried, then rehydrated in PBS at room temperature for 15 minutes. To block nonspecific binding, the tissues were incubated with 2% BSA at room temperature for 30 minutes. Subsequently, the sections were incubated at room temperature for 1 hour with the primary antibody (Table 1), then washed three times in PBS that contained 0.15% Triton

TABLE 1. Primary Antibodies and Source

Antibodies	Category	Dilution	Source
Integrin $\alpha 6$	Mouse monoclonal	$\times 200$	Chemicon, International, Inc. (Temecula, CA)
Integrin $\beta 4$	Mouse monoclonal	$\times 500$	Chemicon, International, Inc.
Integrin $\beta 1$	Mouse monoclonal	$\times 500$	Chemicon, International, Inc.
Collagen IV	Mouse monoclonal	$\times 200$	MP Biomedicals (Eschwege, Germany)
Collagen VII	Mouse monoclonal	$\times 100$	Chemicon, International, Inc.
Laminin 5	Mouse monoclonal	$\times 100$	Chemicon, International, Inc.
Keratin 3	Mouse monoclonal	$\times 50$	Progen (Wieblingen, Germany)
Keratin 4	Mouse monoclonal	$\times 200$	Novocastra (New Castle upon Tyne, UK)
Keratin 12	Goat polyclonal	$\times 100$	Santa Cruz Biotechnology, Inc. (Santa Cruz, CA)
Keratin 13	Mouse monoclonal	$\times 200$	Novocastra

X-100 for 15 minutes. Control incubations were with the appropriate normal mouse and goat IgG (Dako, Kyoto, Japan) at the same concentration as the primary antibody, and omission of the primary antibody for the respective specimen. After staining with the primary antibody, the sections were incubated at room temperature for 1 hour with appropriate secondary antibodies, fluorescein (FITC)-conjugated donkey anti-mouse IgG and FITC-conjugated donkey anti-goat IgG (Molecular Probes, Eugene, OR). After several washings with PBS, the sections were coverslipped by using antifading mounting medium that contained propidium iodide (Vectashield; Vector, Burlingame, CA) and were examined by confocal microscopy (Olympus Fluoview, Tokyo, Japan).

Electron Microscopy

Human donor corneal epithelial cells cultured on denuded amniotic membrane by using AS- or FBS-supplemented media were examined by scanning electron microscopy (SEM) and transmission electron microscopy (TEM). Specimens were fixed in 2.5% glutaraldehyde in 0.1M PBS, washed three times for 15 minutes in PBS and post-fixed for 2 hours in 2% aqueous osmium tetroxide. They were then washed three more times in PBS before being passed through a graded ethanol series (50, 70, 80, 90, 95, and 100%). For SEM preparation, specimens were transferred to hexamethyldisilazane (TAAB Laboratories Equipment Ltd., Berkshire, UK) for 10 minutes and allowed to air-dry. When dry,

the specimens were mounted on aluminum stubs and sputter-coated with gold before examination in a digital SEM (JEOL JSM 5600; Herts, UK). For TEM preparation, the specimens were embedded in epoxy resin (Agar 100-epoxy resin; Agar Scientific, Essex, UK). Ultrathin (70 nm) sections were collected on copper grids and stained for 1 hour with uranyl acetate and 1% phosphotungstic acid, then for 20 minutes with Reynold's lead citrate before examination on a TEM (JEOL JEM 1010).

RESULTS

Proliferative Capacity and Clonal Growth

In both AS- and FBS-supplemented media, human corneal and oral epithelial cells formed colonies with ovoid and round cells, with some elongated cells (Fig. 1). The epithelial morphology of cells cultivated in AS- and FBS-supplemented media was comparatively similar. BrdU proliferation assay showed that the PIs of human corneal epithelium cultivated by using AS and FBS were 3.00 ± 0.16 and 3.10 ± 0.03 , respectively (Fig. 2A). These differences were not statistically significant. The PIs of human oral epithelium cultivated by using AS and FBS were 2.50 ± 0.31 and 2.67 ± 0.16 , respectively (Fig. 2A). These differences were also not statistically significant.

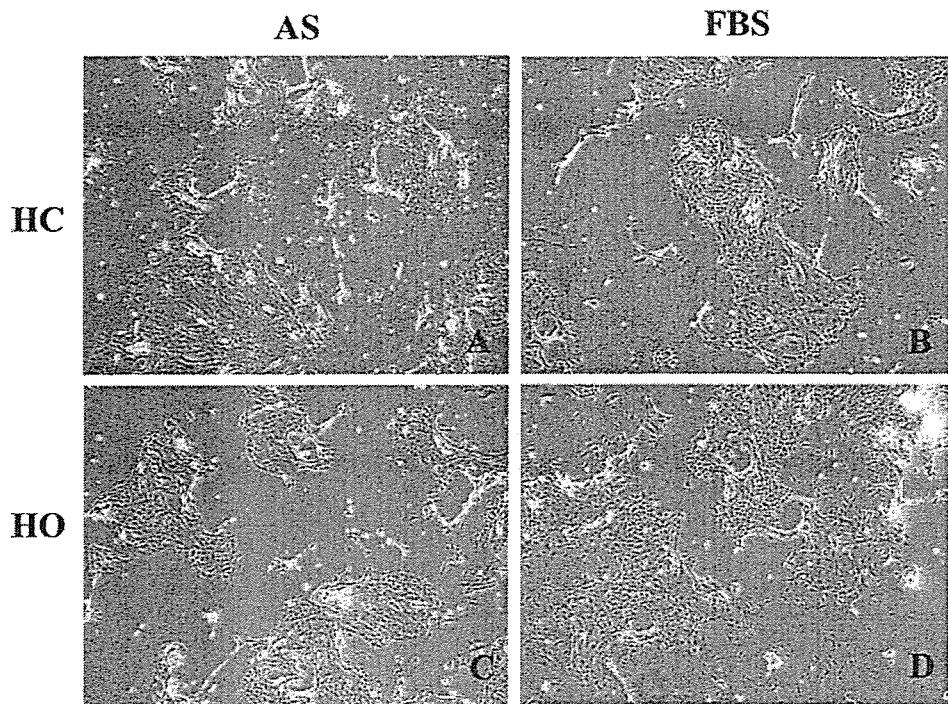


FIGURE 1. Representative phase contrast appearance of human corneal epithelial cells (A, B) and human oral epithelial cells (C, D) cultivated in AS- (A, C) and FBS-supplemented (B, D) media on day 6. In both AS- and FBS-supplemented media, human corneal and oral epithelial cells formed colonies consisting of ovoid and round cells with some elongated cells. The epithelial cell morphology was very similar between the 2 groups. Original magnification, $\times 40$. HC, human corneal epithelium; HO, human oral epithelium.

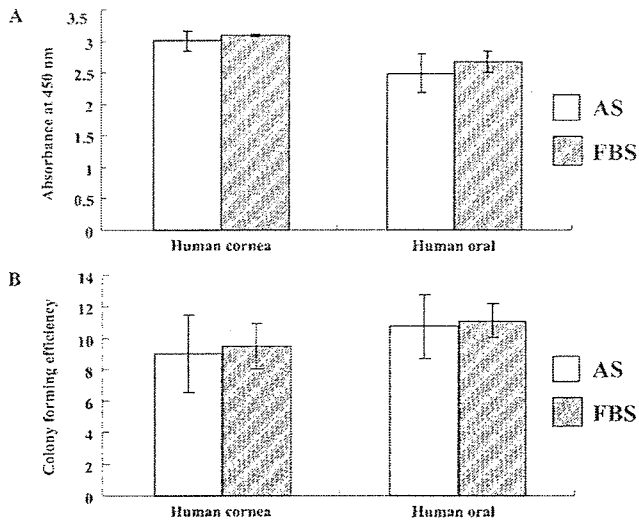


FIGURE 2. (A) BrdU ELISA cell proliferation assay of corneal and oral epithelial cells cultivated in AS- ($n = 12$) and FBS-supplemented ($n = 12$) media. The bars show the mean values of BrdU absorbance in each culture condition. Proliferation indices (PI) of human corneal epithelial cells were 3.00 ± 0.16 (AS) and 3.10 ± 0.03 (FBS), whereas PIs of human oral epithelial cells were 2.50 ± 0.31 (AS) and 2.67 ± 0.16 (FBS). There were no statistically significant differences between them. (B) Colony forming efficiencies (CFE) of human corneal epithelial cells were $9.0 \pm 2.45\%$ (AS) and $9.5 \pm 1.45\%$ (FBS), whereas CFEs of human oral epithelial cells were $10.75 \pm 2.01\%$ (AS) and $11.1 \pm 1.05\%$ (FBS). There were also no statistically significant differences between them.

The CFEs of human corneal epithelial cells were $9.0 \pm 2.45\%$ (AS) and $9.5 \pm 1.45\%$ (FBS), whereas the CFEs of human oral epithelial cells were $10.75 \pm 2.01\%$ (AS) and $11.1 \pm 1.05\%$ (FBS) (Fig. 2B). For both corneal and oral epithelial cells, there were no statistically significant differences between the CFEs of AS- and FBS-supplemented cultures.

Differentiation of Cultivated Corneal and Oral Epithelial Cells

The expression patterns of several tissue-specific keratins in cultivated corneal (Fig. 3) and oral (Fig. 4) epithelium were investigated immunohistochemically. Negative control sections, incubated with normal mouse and goat IgG, and primary antibody omission exhibited no discernible specific immuno-

reactivity over the entire region. The immunoreactivity observed in each specimen was compared with these controls.

In the normal (Figs. 3A3, 3B3) and cultivated (Figs. 3A1, 3A2, 3B1, 3B2) corneal epithelial cells, the cornea-specific keratins 3 and 12 were expressed in the superficial and intermediate layers, with less discernible immunostaining in the basal cell layers. The expression patterns of these keratins were similar between epithelial sheet cultivated by using AS (Figs. 3A1, 3B1) and FBS (Figs. 3A2, 3B2).

In human normal oral epithelium, keratin 3 (Fig. 4A3) and keratin 13 (Fig. 4C3) were expressed in all epithelial layers except basal cell layers; keratin 4 was expressed in the superficial and upper half of intermediate layers (Fig. 4B3). In the cultivated epithelial sheet, keratins 3 and 13 were expressed in almost all epithelial cell layers (Figs. 4A1, 4A2, 4C1, 4C2), whereas keratin 4 was sporadically expressed in the superficial cell layers (Figs. 4B1, 4B2). The expression pattern of these keratins was also similar between epithelial sheets cultivated when using AS (Figs. 4A1, 4B1, 4C1) and FBS (Figs. 4A2, 4B2, 4C2).

Basement Membrane Assembly Protein Expression

Immunohistochemistry showed linearly positive staining of integrin $\alpha 6$ (Figs. 5A1–5A3, Figs. 6A1–6A3), integrin $\beta 4$ (Figs. 5B1–5B3, Figs. 6B1–6B3), collagen IV (Fig. 5D13, Figs. 6D1–6D3), collagen VII (Figs. 5E1–5E3, Figs. 6E1–6E3), and laminin 5 (Figs. 5F1–5F3, Figs. 6F1–6F3) on the basement membrane side of corneal and oral epithelial cells. In contrast, integrin $\beta 1$ was expressed in the cell membrane of epithelial cells (Figs. 5C1–5C3, Figs. 6C1–6C3). These AS- and FBS-derived epithelial sheets maintained the phenotypic characteristics of normal in vivo corneal and oral epithelia.

Electron Microscopy

SEM examination revealed a continuous layer of flat squamous polygonal epithelial cells in corneal epithelial cells cultivated by using AS (Fig. 7A1) and FBS (Fig. 7B1). The cells in both groups were closely attached to each other, with tightly opposed cell junctions and distinct cell boundaries, and the apical surface of the cells was covered with numerous microvilli (Figs. 7A2, 7B2).

TEM examination of the corneal epithelial culture sheet showed that the cells appeared healthy and had differentiated into basal columnar cells, suprabasal cuboid wing cells, and flat squamous superficial cells (Figs. 7A3, 7A4, 7B3, 7B4). The basal

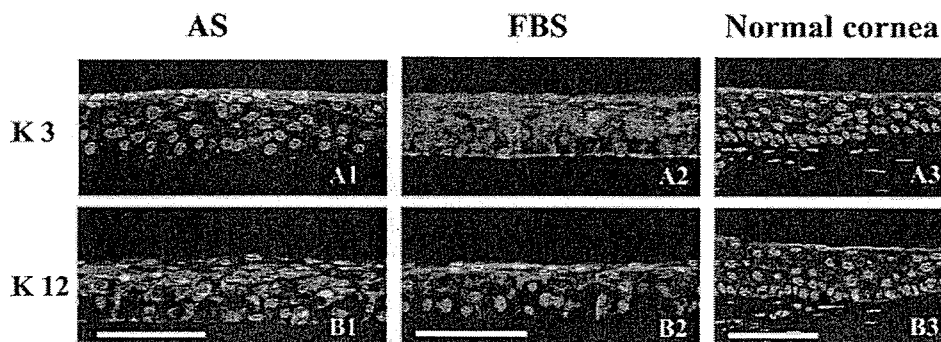


FIGURE 3. Representative immunohistochemical results of cultivated cornea epithelial sheets in AS- (A1, B1) and FBS-supplemented (A2, B2) media, compared with normal in vivo cornea epithelium (A3, B3). In all 3 epithelia, cornea-specific keratins 3 (A1–A3) and 12 (B1–B3) were expressed in the superficial and intermediate layers, with less discernible immunostaining in the basal-cell layers. The expression patterns of these proteins were similar in cultivated epithelial sheets derived from AS- and FBS-supplemented culture systems. Scale bars, 100 μm .

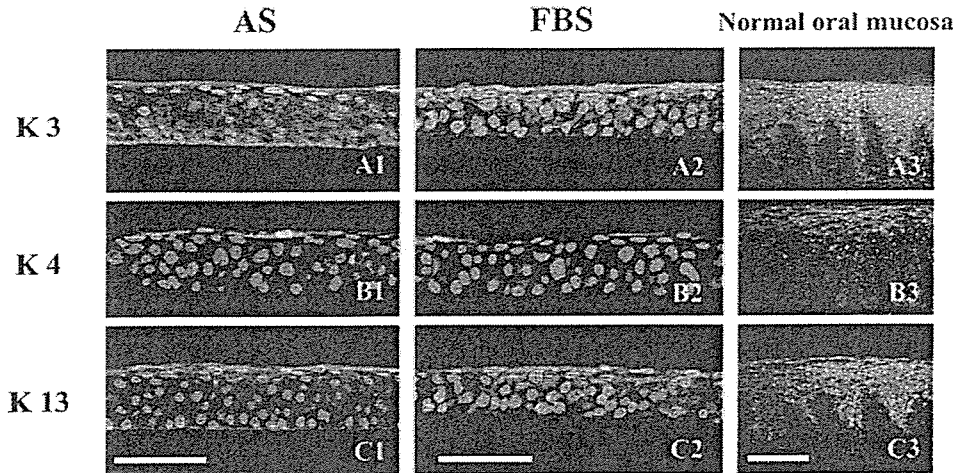


FIGURE 4. Representative immunohistochemical results of cultivated oral epithelial sheets in AS- (A1-C1) and FBS-supplemented (A2-C2) media, compared with normal *in vivo* oral epithelium (A3-C3). In normal oral epithelium, keratin 3 (A3) and keratin 13 (C3) were expressed in all epithelial layers, except the basal-cell layers, and keratin 4 was expressed in the superficial and upper half of the intermediate layer (B3). In the cultivated epithelial sheet, keratins 3 and 13 were expressed in almost all epithelial cell layers (A1, A2, C1, C2), whereas keratin 4 was sporadically expressed in the superficial cell layers (B1, B2). The expression patterns of these proteins were similar in cultivated epithelial sheets derived from AS- and FBS-supplemented culture systems. Scale bars, 100 μ m.

epithelial cells adhered well to the AM substrate with hemidesmosome attachments, and produced basement membrane material (Figs. 7A5, 7B5). In all cell layers, the epithelial cells were

comparatively closely attached to neighboring cells by numerous desmosomal junctions (Figs. 7A6, 7B6). Morphologic patterns were similar between AS- and FBS-culture systems.

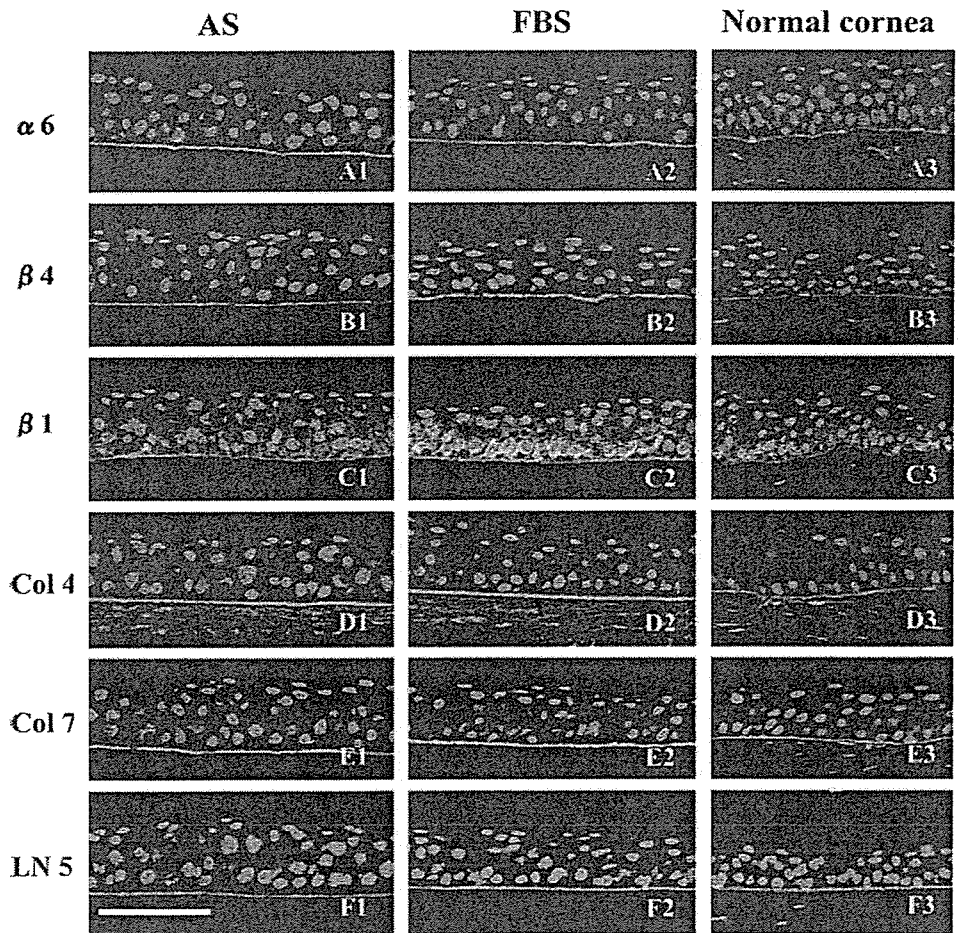


FIGURE 5. Representative immunohistochemical results of cultivated cornea epithelial sheets in AS- (A1-F1) and FBS-supplemented (A2-F2) media, compared with normal *in vivo* cornea epithelium (A3-F3). There was linear positive staining of integrin $\alpha 6$ (A1-A3), integrin $\beta 4$ (B1-B3), collagen IV (D1-D3), collagen VII (E1-E3), laminin 5 (F1-F3) on the basement membrane side of cultivated corneal epithelial cells, similar to that of normal corneal epithelium. In contrast, integrin $\beta 1$ was expressed in the cell membrane of epithelial cells (C1-C3). The expression patterns of these proteins were similar in cultivated epithelial sheets derived from AS- and FBS-supplemented culture systems. Scale bars, 100 μ m.

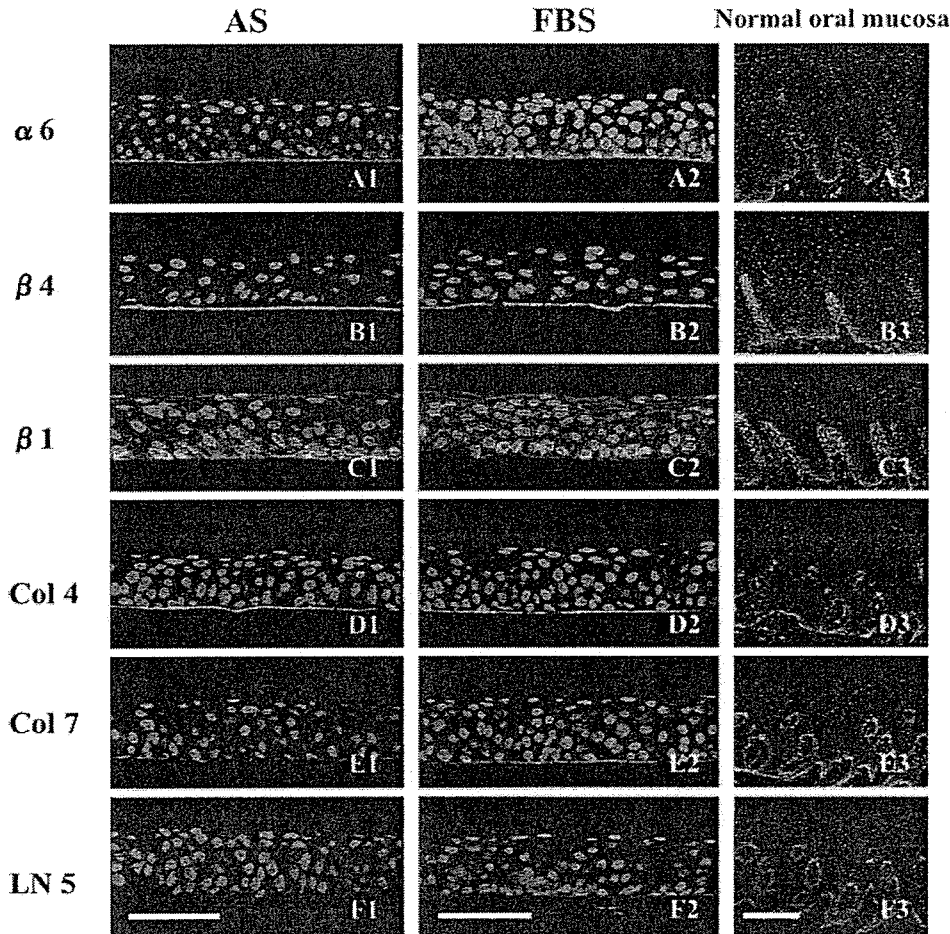


FIGURE 6. Representative immunohistochemical results of cultivated oral epithelial sheets in AS- (A1-F1) and FBS-supplemented (A2-F2) media, compared with normal *in vivo* oral epithelium (A3-F3). There was linear positive staining of integrin $\alpha 6$ (A1-A3), integrin $\beta 4$ (B1-B3), collagen IV (D1-D3), collagen VII (E1-E3), laminin 5 (F1-F3) on the basement membrane side of cultivated oral epithelial cells, similar to that of normal oral epithelium. In contrast, integrin $\beta 1$ was expressed in the cell membrane of epithelial cells (C1-C3). The expression patterns of these proteins were similar in cultivated epithelial sheets derived from AS- and FBS-supplemented culture systems. Scale bars, 100 μm .

DISCUSSION

Previous studies on cultivated ocular tissue equivalents have relied primarily on bovine serum-supplemented media.⁶⁻⁸ However, the use of FBS in the culture system is a major concern, because BSE cannot be detected by any known *in vitro* assay. Cultivated ocular surface epithelial transplantation has mainly been used for treating various severe OSDs where conventional therapy has had limited success. As such, the use of AS for the development of bioengineered ocular surface equivalents would be of particular clinical relevance in these patients. We demonstrate for the first time that AS-supplemented media derived from patients with SJS were able to support epithelial-cell propagation, as well as the development of tissue-equivalents bearing similar morphologic and ultrastructural characteristics as the normal *in vivo* tissues.

Previous reports on epithelial equivalents have mainly focused on obtaining differentiated, stratified tissue equivalents.²²⁻²⁵ However, the ability of culture media to support the proliferation of cells is a critical issue in propagating cells for clinical transplantation, if these cells are to continue to regenerate the tissue of origin.^{19,25} It has previously been demonstrated that cells cultivated by using human serum from normal patients supported the *in vitro* and *in vivo* proliferation of human conjunctival epithelial cells.¹⁵ SJS is a major cause of severe OSD, and afflicted patients often have multisystemic involvement. In our study, we addressed the critical issue of whether AS-supplemented media from these SJS patients were able to support *in vitro* cell proliferation as effectively as conventional bovine serum-supplemented media. By using

BrdU-ELISA proliferation assays, as well as clonal growth studies, we showed that human corneal and oral epithelial cells cultivated in AS-supplemented media had *in vitro* capacities comparable with those of conventional FBS supplemented media. These findings are important in supporting the use of AS for the *ex vivo* expansion of epithelial cells.

We further demonstrated that these AS-derived cultivated corneal and oral epithelial cells formed confluent stratified epithelial sheets on AM. The histologic appearance of these epithelial sheets closely resembled the tissue of origin in terms of cell morphology, as well as degree of stratification. Ultrastructural examination of the epithelial equivalents cultivated in AS- and FBS-supplemented media revealed the presence of well-formed, multilayered epithelial sheets with tightly opposed cell junctions. The apical surface of the cultivated oral epithelial cells was covered with numerous microvilli, which was almost identical with that found in *in vivo* corneal epithelium. In both AS- and FBS-supplemented culture systems, cultivated corneal and oral epithelial cells each retained their innate phenotypic characteristics, as confirmed by their expression of tissue-specific keratins. These findings demonstrate the ability of AS-supplemented culture media to support the continued proliferation and differentiation of cultivated cells in bioengineered tissue equivalents, which is of paramount importance when considering its use in clinical transplantation.

A critical issue regarding the use of cultivated epithelial sheets for ocular surface reconstruction is the ability of these tissue equivalents to retain their structural integrity after transplantation. This is dependent on basal-cell attachments to the underlying substrate, as well as cell-to-cell adhesion structures.